THESIS FOR THE DEGREE OF DOCTOR OF PHILOSOPHY

# Studies of the Selective Catalytic Reduction of Nitrogen Oxides with Dimethyl Ether

STEFANIE TAMM

Department of Chemical and Biological Engineering

CHALMERS UNIVERSITY OF TECHNOLOGY

Göteborg, Sweden 2010

Studies of the Selective Catalytic Reduction of Nitrogen Oxides with Dimethyl Ether
STEFANIE TAMM
ISBN 978-91-7385-389-7



Doktorsavhandlingar vid Institutionen för kemi- och bioteknik
Chalmers tekniska högskola
Serie nr. 2010: 3070
ISSN 0346-718X

Department of Chemical and Biological Engineering
Chalmers University of Technology
SE-412 96 Göteborg
Sweden
Telephone: +46 – (0)31 – 772 1000

Cover:
Illustration of surface species present during DME-SCR over $\gamma$-$Al_2O_3$.

Chalmers Reproservice
Göteborg, Sweden 2010

**Studies of the Selective Catalytic Reduction of Nitrogen Oxides with Dimethyl Ether**

STEFANIE TAMM
Department of Chemical and Biological Engineering
Chalmers University of Technology

ABSTRACT

Dimethyl ether (DME) is one of the most energy-efficient and low $CO_2$ emitting alternative fuels when produced from biomass. Similar to other vehicles with combustion engines, vehicles running on DME will most likely need after-treatment technologies for the reduction of $NO_x$ emissions to meet the most stringent upcoming legislations. One attractive technique would be selective catalytic reduction with DME as reducing agent (DME-SCR), which is in the focus of this thesis.

The activity for $NO_x$ reduction with DME of several acidic catalysts was studied in a flow reactor and the accumulation and consumption of surface species was monitored in diffuse reflectance infrared Fourier transform (DRIFT) and transmission FTIR spectroscopy experiments over $\gamma$-$Al_2O_3$.

It was shown that dimethyl ether is a special reducing agent since it induces radical reactions in the presence of $O_2$ and NO above 300 °C before the catalyst, with $NO_2$ and CO as the main products. Despite the changed feed gas composition, activity tests with DME as reducing agent in the flow reactor over a zeolite H-ZSM-5 and a $\gamma$-$Al_2O_3$ catalyst resulted in 28 and 47 % $NO_x$ reduction, respectively. During DRIFT and transmission FTIR spectroscopy experiments, methoxy, formate, nitrate, nitrite, NCO and likely formohydroxamic acid and formaldehyde-like species were observed on the $\gamma$-$Al_2O_3$ surface. A reaction mechanism which explains the involvement of these species in the selective catalytic reduction of $NO_x$ was proposed.

For DME-SCR over $\gamma$-$Al_2O_3$ it was shown in experiments where the occurrence of the gas phase reactions could be controlled independently of the catalyst temperature, that the formation of $NO_2$ in the gas phase reactions boosts the activity for $NO_x$ reduction at 250 °C, probably due to a more efficient reaction with NCO surface species. In contrast, at 350 °C, lower activity for $NO_x$ reduction was observed in the presence than in the absence of gas phase reactions. This negative effect was explained by partial oxidation of DME in the gas phase reactions partly consuming the limiting reducing agent at 350 °C.

**Keywords**: DME, lean de$NO_x$, reaction mechanism, $NO_2$ formation, gas phase reaction, acidic zeolite, isocyanate

**Studier av den selektiva katalytiska reduktionen av kväveoxider med dimetyl eter**

STEFANIE TAMM
Institution för kemi- och bioteknik
Chalmers Tekniska Högskola

SAMMANFATTNING

Dimetyleter (DME) är ett av de mest energieffektiva alternativa bränslena om den framställs från biomassa. Som bränsle är DME mest intressant för dieselprocessen på grund av sitt höga cetantal. Likt andra fordon med förbränningsmotor, kommer fordon med DME-motorer behöva avgasreningssystem för att klara de striktaste lagkraven för kväveoxidutsläppsgränser. En intressant teknik för reduktion av kväveoxider ur avgaser med syreöverskott är den kontinuerliga katalytiskt selektiva $NO_x$-reduktionen med DME som avhandlingen fokuserar på.

Aktiviteten för $NO_x$-reduktion studerades i första hand för H-ZSM-5 och $\gamma$-$Al_2O_3$ katalysatorer i en flödesreaktor. Ackumuleringen och förbrukningen av ytföreningar på $\gamma$-$Al_2O_3$ följdes med DRIFT (diffuse reflectance infrared Fourier transform) och transmissions FTIR spektroskopi.

Det visades att DME är ett mycket speciellt reduktionsmedel i och med att den dissocierar i gasfasen före katalysatorn till radikaler. Över 300 °C startar reaktioner i närvaro av syre och NO, som huvudsakligen leder till $NO_2$ och CO. Trots dessa förändringar i reduktionsmedlet visar H-ZSM-5 med 28 % och $\gamma$-$Al_2O_3$ med 47 % bra aktivitet för $NO_x$-reduktion i en flödesreaktor. I DRIFT- och transmissions FTIR-experiment iakttogs metoxy-, format-, nitrat-, nitrit-, NCO- och troligen CHO-N(H)OH och formaldehydliknande föreningar på $\gamma$-$Al_2O_3$-ytan. En reaktionsmekanism som förklarar dessa föreningars deltagande i den selektiva katalytiska $NO_x$-reduktionen med DME föreslogs.

I experiment där förekomsten av gasfasreaktionerna kunde styras oberoende av katalysatortemperaturen kunde det visas att $NO_2$-bildningen i gasfasreaktionerna förbättrar $NO_x$-reduktionen med DME över $\gamma$-$Al_2O_3$ vid 250 °C. Detta sker troligen på grund av en mer effektiv reaktion med NCO-ytföreningar. Å andra sidan var $NO_x$-reduktionen vid 350 °C lägre vid närvaro än vid frånvaro av gasfasreaktionerna. Denna negativa effekt förklarades med en partiell oxidation av DME i gasfasreaktionerna som leder till en minskad tillgång till det begränsande reduktionsmedlet. Experiment DRIFT-spectroscopi visade dessutom att isocyanater är viktiga mellanprodukter i reaktionsmekanismen på en $\gamma$-$Al_2O_3$ katalysator.

## LIST OF PUBLICATIONS

This thesis is based on the work contained in the following papers, referred to by Roman numerals in the text:

**I.** "On the different roles of isocyanate and cyanide species in propene-SCR over silver/alumina", Stefanie Tamm, Hanna Härelind Ingelsten and Anders E. C. Palmqvist, *Journal of Catalysis,* 255, 2008, pp. 304-312.

**II.** "DME as reductant for continuous lean reduction of $NO_x$ over ZSM-5 catalysts", Stefanie Tamm, Hanna H. Ingelsten and Anders E. C. Palmqvist, *Catalysis Letters,* 123, 2008, pp. 233-238.

**III.** "The influence of gas phase reactions on the design criteria for catalysts for lean $NO_x$ reduction with dimethyl ether", Stefanie Tamm, Hanna H. Ingelsten, Magnus Skoglundh and Anders E. C. Palmqvist, *Applied Catalysis B: Environmental,* 91, 2009, pp. 324-241.

**IV.** "Differences between $Al_2O_3$ and $Ag/Al_2O_3$ for lean reduction of $NO_x$ with dimethyl ether", Stefanie Tamm, Hanna H. Ingelsten, Magnus Skoglundh and Anders E. C. Palmqvist, *Topics in Catalysis*, 52, 2009, pp. 1813-1816.

**V.** "Mechanistic aspects of the selective catalytic reduction of $NO_x$ by dimethyl ether and methanol over $\gamma$-$Al_2O_3$ ", Stefanie Tamm, Hanna H. Ingelsten, Magnus Skoglundh and Anders E. C. Palmqvist, *submitted to Journal of Catalysis*

**VI.** "Influence of gas phase reactions on DME-SCR over $\gamma$-alumina", Stefanie Tamm, Hanna H. Ingelsten, and Anders E. C. Palmqvist, *submitted to Journal of Catalysis*

## CONTRIBUTION REPORT

**I.** I prepared the catalysts, performed the flow reactor and some of the DRIFT experiments, interpreted the results together with my co-authors and was responsible for writing and submitting the paper.

**II.** I prepared the catalysts, performed the flow reactor experiments, interpreted the results together with my co-authors and was responsible for writing and submitting the paper.

**III.** I performed the flow reactor experiments, interpreted the results with input of my co-authors and was responsible for writing and submitting the paper.

**IV.** I prepared the catalysts, performed the flow reactor experiments, interpreted the results with input of my co-authors and was responsible for writing and submitting the paper.

**V.** I performed the DRIFT experiments, interpreted the results with input of my co-authors and was responsible for writing and submitting the paper.

**VI.** I made-up the experimental set-up and discussed it with my co-authors, performed the activity tests and the transmission IR experiments, interpreted the results with input of my co-authors and was responsible for writing and submitting the paper.

# Contents

# 1. Introduction

Global warming as a result of the greenhouse effect has obtained increasing attention during the last years. Already in 1997, an agreement was reached in the Kyoto protocol, which commits 37 industrialized countries and the European Union to reduce their greenhouse gas emissions with five percent compared to 1990 in the period of 2008 until 2012 [1]. The objective for an agreement for the years after 2012 is to stabilize the greenhouse gas concentrations in the atmosphere until 2050 at such a level that the increase in global temperature stays below 2 °C as declared on COP 15 [2]. One of the greenhouse gases whose emissions need to be reduced in the future to reach this goal is carbon dioxide ($CO_2$). Road transportation is an important source of $CO_2$ through the combustion of fuel in the engines. One way to decrease the $CO_2$ emissions is the use of so called lean burn engines, like diesel engines and lean burn gasoline engines. These engines operate with excess oxygen, which facilitates a better utilisation of the energy stored in the fuel. A further reduction of the $CO_2$ emissions can be achieved by running these engines on alternative fuels from renewable sources. Examples of such alternative fuels are biogas, ethanol, methanol, different diesel substitutes such as Fischer-Tropsch diesel or vegetable oil-based diesel, hydrogen ($H_2$) and DME. The potential for $CO_2$ reduction, however, differs considerably for these alternative fuels. One of the most energy effective and low $CO_2$ emitting alternative fuels is DME when produced from biomass as shown in well-to-wheel studies [3, 4].

## *1.1. DME as an alternative fuel*

Dimethyl ether (DME) has the chemical formula $CH_3$-O-$CH_3$ and the IUPAC name methoxymethane. It is environmentally benign, since it has a low global warming potential and is, moreover, neither toxic, mutagenic, carcinogenic nor teratogenic, in contrast to conventional fuels [5]. Dimethyl ether has been used for various applications for about 40 years, mainly as a propellant in aerosol products like hair and paint spray, replacing CFC as a refrigerant, as a (co-)blowing agent for foam, as a solvent, and as an extraction agent [6, 7]. For these applications, it has been mainly produced by dehydration of methanol [6], but in view of the interest in DME as a fuel, single plant processes for DME production from synthesis gas have been developed [7, 8]. Dimethyl ether has more well defined properties compared to

conventional gasoline or diesel, and, moreover, does not contain sulphur or aromatic hydrocarbons.

One property which qualifies DME as an interesting alternative fuel for the use in diesel engines is its high cetane number of 55-60 [3, 5], which is only slightly higher than that of diesel. In a diesel engine, DME has the further advantage that virtually no soot is produced during its combustion [5, 9]. Moreover, DME can be liquefied under low overpressure (> 5 bar) and, therefore, handled the same way as liquefied petroleum gas (LPG) partly using existing infrastructure [5, 9], which facilitates the market introduction of DME as a fuel.

## *1.2. Reduction of nitrogen oxides in mobile applications*

The formation of nitrogen oxides ($NO_x$) is during the combustion of fuel in an engine a generic problem [10, 11] since nitrogen oxides are toxic, contribute to acid rain and the formation of tropospheric ozone [10-13]. Therefore, the emissions of $NO_x$ have been regulated in many countries and the limits of these regulations have been stepwise made stricter during the last two decades as shown in Figure 1.1. Moreover limits have been introduced in an increasing number of countries all over the world as illustrated in Figure 1.2 [14, 15]. The $NO_x$ emissions can be lowered by various engine measures and through exhaust gas recirculation (EGR). The level of

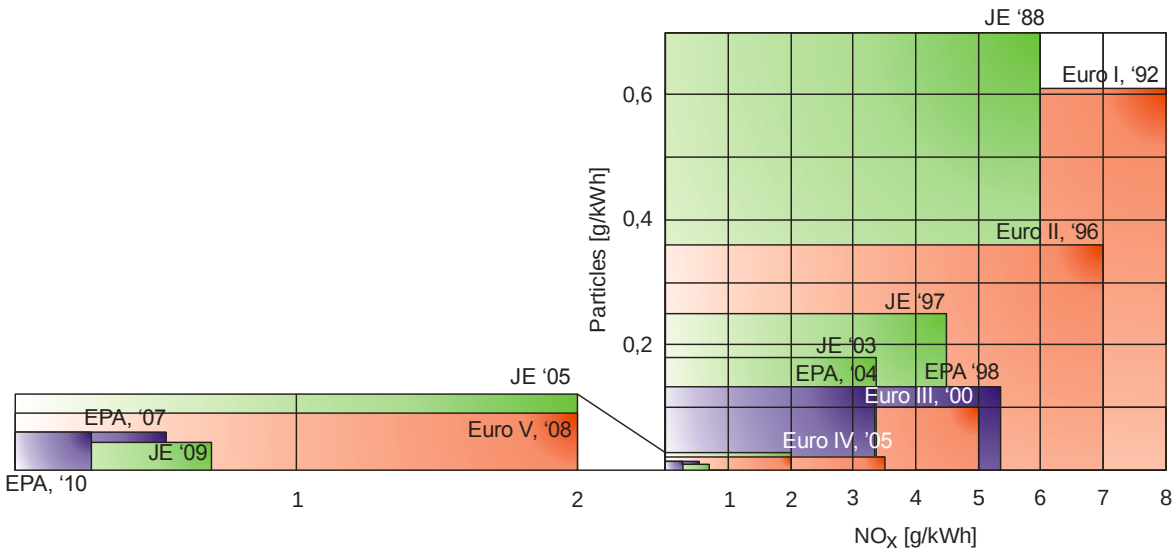


**Figure 1.1:** Emission regulations for $NO_x$ and particles in the European Union, the USA and Japan for heavy duty engines at different years, based on data from [15, 16].

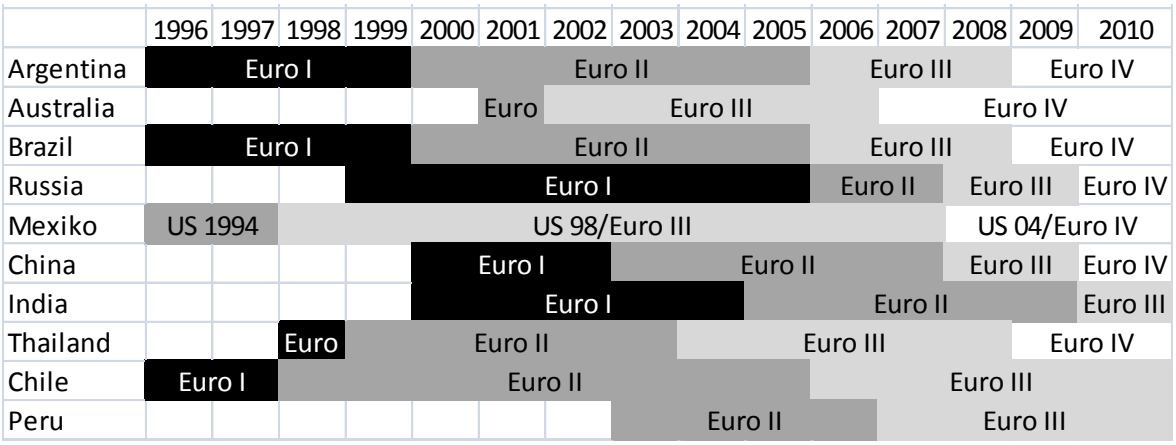


**Figure 1.2: E**xamples for implementation of stricter emission regulations for heavy duty engines during the last years in several countries, based on data from [15].

EGR that can be employed depends partly on the amount of particulate matter generated during combustion and compared to diesel fuel higher EGR rates can be applied with DME. This gives DME combustion the additional advantage of lower $NO_x$ emissions. Today, however, exhaust gas after-treatment systems are typically needed in order to reach the most stringent emission limits.

A proven concept for reducing $NO_x$ for vehicles is the three-way catalyst (TWC). Over this type of catalytic converter, $NO_x$ is efficiently reduced to $N_2$ under stoichiometric redox conditions as illustrated in Figure 1.3. At the appropriate air/fuel ratio, unburned or partly burned fuel and CO are simultaneously oxidized to $CO_2$ and water reaching conversions over 90 % for all these reactions. However, in the presence of excess oxygen as in the exhaust from diesel or lean burn gasoline engines, the activity for $NO_x$ reduction over the TWC decreases dramatically as illustrated in Figure 1.3.

In excess oxygen, the most attractive way to reduce $NO_x$ would be through thermal decomposition of $NO_x$ into $N_2$ and $O_2$, which is indeed thermodynamically favourable at typical exhaust gas temperatures but severely kinetically limited. In the literature, the zeolite Cu-ZSM-5 is reported to be the most promising catalyst for NO decomposition due to its capacity to desorb oxygen at high temperature [17]. However, the presence of oxygen hinders the catalytic decomposition so that no efficient decomposition catalyst has been commercialized in practical applications [17, 18].

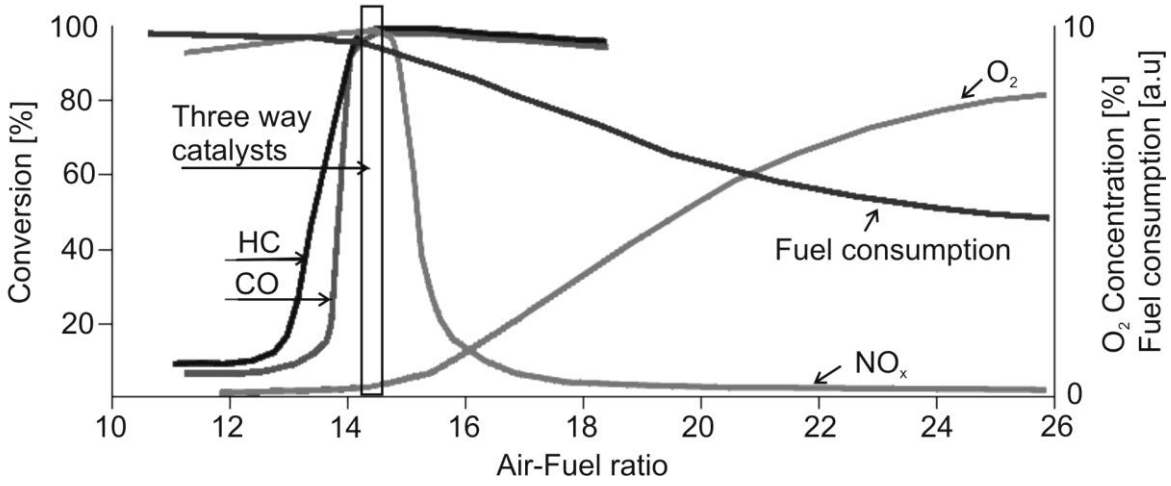


**Figure 1.3:** Oxygen concentration, fuel consumption and conversion of $NO_x$, hydrocarbons and CO over a three-way catalyst, as a function of the air to fuel-ratio. An air to fuel-ratio of 14.6 corresponds to stoichiometric operation. Figure adopted from [19].

Therefore, mainly three other concepts have been developed for $NO_x$ reduction in excess oxygen. The first concept is the $NO_x$ storage and reduction catalyst (NSR), which is based on Pt, Pd and Rh as active metals for $NO_x$ reduction and Ba as $NO_x$ storage material [20]. Under normal driving conditions, the engine runs lean (in excess oxygen) and nitrogen oxides are stored on the catalyst. When the storage capacity is exhausted, the stored $NO_x$ is reduced intermittently under short periods, while the engine is operated rich (oxygen deficient), and the catalyst is regenerated. The main benefit of this technique is its high $NO_x$ conversion. The drawbacks of this concept, however, are high costs for the high precious metal loadings, sulphur sensitivity and the necessity to obtain a rich exhaust gas with a lean burn engine. In the context of this thesis it is worth to notice, that more than 90 % $NO_x$ conversion has been achieved over a commercial NSR catalyst with DME as reducing agent [21].

The second catalyst concept is the continuous reduction of $NO_x$ with ammonia ($NH_3$), called ammonia-assisted selective catalytic reduction (ammonia-SCR). This technique has successfully been used in power plants for many years. Since ammonia is both caustic and hazardous, its storage is not suitable in mobile applications. Therefore, an aqueous solution of urea is used instead, which is hydrolysed at high temperatures to $NH_3$ and $CO_2$. Ammonia-SCR is the most efficient technique available today to reduce $NO_x$ in excess oxygen and is now

implemented in modern trucks. The main principle drawback of this technique is the need for an additional liquid that the vehicle has to be fuelled with.

The third concept is the hydrocarbon-assisted selective catalytic reduction (HC-SCR) of $NO_x$, also known as lean de$NO_x$ or lean $NO_x$ catalyst (LNC). In HC-SCR, the $NO_x$ is continuously reduced by unburned or partially oxidized fuel in excess oxygen. This concept is most desirable from a vehicle system viewpoint and at the same time most comfortable from a driver's viewpoint. More research, however, is needed to enhance $NO_x$ conversion efficiency, durability of the materials and in some cases also sulphur and aromatics tolerance. Chapter 2 deals with HC-SCR in more detail.

## *1.3. Objective*

The introduction of DME as an alternative fuel in mobile applications appears to be desirable in view of the $CO_2$ emissions. Similar to any other fuel, the combustion of DME in the engine of such a DME fuelled vehicle will form $NO_x$, which needs to be reduced to satisfy the most stringent legislations. The selective catalytic reduction of $NO_x$ with DME appears in such a scenario to be an interesting solution for the problem. The objective of this study is thus to find a suitable catalyst for DME-SCR, to explain the particularities of DME compared to other carbon containing reducing agents and to propose a reaction mechanism for DME-SCR.

# 2. Selective catalytic reduction of $NO_x$ with hydrocarbons

Ritscher and Sander patented in 1981 a copper containing zeolite catalyst, which was able to reduce $NO_x$ with hydrocarbons in the presence of excess oxygen [22]. In the late 1980s, Iwamoto et al. and Held et al. independently reported that copper exchanged ZSM-5 (Cu-ZSM-5) catalysts are active for the selective catalytic reduction of $NO_x$ with hydrocarbons [23, 24]. During the following years, it was found that several precious metals, metal oxides, promoted metal oxides and zeolites also are active for lean $NO_x$ reduction with hydrocarbons and other carbon containing reducing agents such as alcohols [25-27]. In contrast to $NO_x$ reduction over a three-way catalyst, where the reduction is hampered by excess oxygen, the selective catalytic reduction with hydrocarbons is promoted by $O_2$ [28]. This leads to a typical volcano shaped curve for the $NO_x$ conversion activity versus temperature. Increasing conversion with temperature is due to faster reactions and, thus, activation of more reducing agent. The decrease in $NO_x$ reduction above the optimum temperature is ascribed to competitive reactions between NO and $O_2$ for the reductant. The non-selective combustion of the reducing agent with $O_2$ becomes faster than reduction of $NO_x$ by the reducing agent at higher temperatures and diminishes, thus, its amount remaining for the SCR reaction. The temperature of maximum $NO_x$ reduction corresponds often to about 90 % conversion of the reducing agent [25].

Pure γ-alumina, which is one of the most thoroughly investigated catalysts in this thesis, has been reported to be active for HC-SCR at high temperatures [25, 29]. In the literature, however, $Al_2O_3$ catalysts have rarely been the main subject for investigations, but served rather as a simpler case to compare the obtained results with [26, 29-35]. In view of the observed similarities between low loaded $Ag/Al_2O_3$ and $\gamma$-$Al_2O_3$, these materials will receive special attention in chapter 2.2. The similarities and differences between catalysts will also be the subject of chapter 2.3 which gives a broad overview over reaction mechanisms depending on type of catalyst. However, not all catalysts are suitable for DME-SCR as will be shown in the next chapter.

## *2.1. DME-SCR*

The literature concerning DME as reducing agent for the selective catalytic reduction of $NO_x$ is quite limited. However, as shown in this thesis, DME is a very special reducing agent which considerably differs from most other carbon-containing reducing agents studied in this context. The activity for $NO_x$ reduction with DME is low over the catalysts that have shown the highest activity for conventional hydrocarbon-SCR: Over a commercial Cu-ZSM-5 based catalyst, the $NO_x$ conversion never reached 5 % in the presence of water [21] and over a $Ag/Al_2O_3$ catalyst the conversion stayed below 20 % [36]. Intermediate activity for $NO_x$ reduction was reported for Ag/mordenite, Ag/ZSM-5, $V_2O_5/Al_2O_3$ and $Ga_2O_3/Al_2O_3$, reaching 25 %, 28 %, 31 % and 35 %, respectively [30, 36, 37]; and the highest conversion has been observed over, $\gamma$-$Al_2O_3$, $Mo/Al_2O_3$, $Sn/Al_2O_3$ and $Co/Al_2O_3$ with 68 %, 71 %, ca 70 %, and ca. 85 %, respectively [30, 38]. However, a direct comparison of the achieved conversion is intricate, due to differing reaction conditions. Higher conversions can be achieved over powder catalysts compared to monolith catalysts due to more active catalytic material per volume. An increase in the $DME/NO_x$ ratio can increase $NO_x$ conversion as shown in **papers II** and **III**. Finally, the presence of water and an increase in space velocity often decreases $NO_x$ conversion [25, 37].

Specific for DME-SCR is the formation of substantial amounts of methanol and formaldehyde as byproducts [30, 38]. On a $\gamma$-$Al_2O_3$ catalyst surface, it has been reported that DME adsorbs dissociatively as methoxy groups ($-O-CH_3$) at 30 °C, as observed by diffuse reflectance Fourier transformed infrared (DRIFT) spectroscopy [39]. Another peculiar feature for DME as reducing agent is that $NO_x$ reduction does not decrease in the presence of water over $Ga_2O_3/Al_2O_3$ in contrast to several hydrocarbons. This observation was explained by the same amount of adsorbed DME in the absence and presence of water [37]. The same surface species as during DME adsorption are also observed when adsorbing methanol over $Al_2O_3$ [40]. These similarities can possibly explain the similar activity in $NO_x$ conversion over $Co/Al_2O_3$ (high conversion) and $Ag/Al_2O_3$ (low conversion) with methanol and DME [36, 38, 41, 42].

## 2.2. $Ag/Al_2O_3$ as HC-SCR catalyst

Since similarities between $\gamma$-$Al_2O_3$ and low loaded $Ag/Al_2O_3$ catalysts have been reported [25, 29], low loaded $Ag/Al_2O_3$ is of interest as a reference for DME-SCR over $\gamma$-$Al_2O_3$, in view of the sparse information available on DME-SCR. These similarities will be discussed in more detail with the reaction mechanism in chapter 2.3.

Alumina promoted by silver is a relatively inexpensive and durable catalyst for the selective catalytic reduction of $NO_x$ with hydrocarbons. High selectivity to $N_2$ is achieved during $NO_x$ reduction over low loaded $Ag/Al_2O_3$ catalysts distinct from high loaded $Ag/Al_2O_3$ catalysts [25, 29, 43]. In general, highest activity for $NO_x$ reduction was achieved at low silver loadings of around 2 wt-% [25, 26, 29, 44-47]. Over these catalysts it has been suggested that dispersed $Ag^+$ ions, small silver oxide clusters and/or silver aluminates prevail [25, 35, 48]. However, the exact nature of the active silver species is still under debate. In view of the nature of the reducing agent it has been shown that the activity for $NO_x$ reduction increases with the chain length of straight hydrocarbons [43]. Moreover, $Ag/Al_2O_3$ is active for $NO_x$ reduction with several oxygenated hydrocarbons, especially ethanol [26, 47, 49-51]. The presence of several percent of water induces a significant decrease in $NO_x$ reduction when using light alkanes or alkenes as reductants, however, high activity can be maintained when oxygenated molecules or long straight hydrocarbons are used [25, 43, 47, 52]. Less important in the context of this thesis are the known issues of $Ag/Al_2O_3$ catalyst deactivation in the presence of sulfur [53, 54] and the decreased activity in the presence of aromatic compounds [55].

## 2.3. Reaction mechanisms

The reaction mechanisms of selective catalytic reduction of $NO_x$ with hydrocarbons discussed in the literature differ depending on the catalyst material and on the reducing agent. However, because of similarities between the mechanisms, they can be grouped into three categories characterized by the nature of the first step of the reaction as proposed in the literature: i) reaction mechanisms starting with NO dissociation, ii) reaction mechanisms with NO oxidation to $NO_2$ as a first step, followed by hydrocarbon activation by $NO_2$, and iii) mechanisms based on parallel activation of $NO_x$ and the reducing agent [18, 56, 57].

### 2.3.1. NO dissociation

The simplest mechanism has been proposed for precious metals supported on oxides such as $Al_2O_3$ [25]. In this mechanism NO adsorbs on the reduced precious metal surface and dissociates into adsorbed N and O species. The combination of two N species results in the formation of $N_2$, while the combination of N with NO gives $N_2O$. The role of the reducing agent is to remove adsorbed O species from the surface and to keep the precious metal in a reduced state [25]. However this reaction mechanism is only applicable for strongly adsorbing hydrocarbons such as propene or higher alkenes, which can adsorb on platinum particles even in excess oxygen [25]. A similar mechanism has been proposed for metal silicates with the difference that only parts of the metals need to be in a reduced state [57].

A related reaction mechanism which starts by NO and CO dissociation has recently been reported for silver particles supported on $Al_2O_3$. By heating the catalyst with a femtosecond laser and following the formation of surface species by nanosecond time-resolved in situ Fourier-transform infrared spectroscopy it could be shown that dissociated C- and N-species on the silver particles form cyanide species. These CN species can flip over to be bound to Al atoms and become oxidized to NCO species as schematically shown in Figure 2.1 [58].

### 2.3.2. NO oxidation to $NO_2$

In contrast to the previously discussed reaction mechanism, platinum particles are reported to be in an oxidized state when using propane as reducing agent [25]. In this case NO cannot dissociate on the platinum particles. Moreover, since $NO_x$ conversion is higher over $Pt/Al_2O_3$ than over $\gamma$-$Al_2O_3$ between 250 and 450 °C [59],

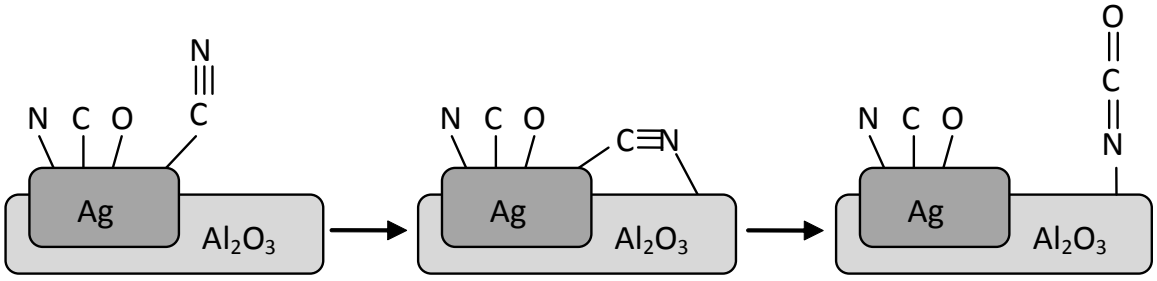


**Figure 2.1:** Proposed formation of NCO species from CN species over $Ag/Al_2O_3$ reproduced from [58].

the reaction mechanism for $NO_x$ reduction is different. This higher catalytic activity of $Pt/Al_2O_3$ has been ascribed to the oxidation of NO to $NO_2$ over platinum [60] and successive reaction steps on both platinum and the alumina support have been proposed [59]. Moreover, it was reported that NO is oxidized to $NO_2$ over dispersed Co species, explaining why the maximum in $NO_x$ reduction with NO was higher over $CoO/Al_2O_3$ than over $\gamma$-$Al_2O_3$, while the opposite was observed with $NO_2$ [33]. This view is supported by a higher activity for $NO_x$ reduction with $NO_2$ than with NO over $Al_2O_3$ as well as over zeolite based catalysts [28, 29, 31, 33, 56].

Based on the previous observations for zeolite based catalysts, a common view is that NO needs to be oxidized to $NO_2$ in a first step [18, 56]. The formed $NO_2$ reacts with NO over an acidic site of a zeolite to two $NO^+$ species and water [61]. These $NO^+$ species may react with the reducing agent to an intermediate containing carbon and nitrogen atoms, which in turn reacts with a further NO or $NO_2$ giving $N_2$ [57].

Other proposed mechanisms which start with the oxidation of NO to $NO_2$ take into account that atoms or groups of atoms with one or more unpaired electrons are radicals according to the IUPAC definition [62]. This implies that $NO^\bullet$ and $NO_2^\bullet$ need to be considered as radicals. For methane it has been suggested that $NO_2^\bullet$ reacts with methane giving $HNO_2$ and a $CH_3^\bullet$ radical according to reaction (2.1) [57].

$$NO_2^\bullet + CH_4 \rightarrow HNO_2 + CH_3^\bullet \qquad (2.1)$$

The $CH_3^\bullet$ radicals may then react with NO and/or $NO_2$ and form C and N containing intermediates. These intermediates are suggested to continue reacting in a similar reaction mechanism as proposed for other reducing agents [57] and will be discussed in the following chapter.

## *2.4. Activation of $NO_x$ and reducing agent*

Most of the reaction mechanisms that assume an activation of both $NO_x$ and the reducing agent are based on observations from FTIR studies. Nitrates ($NO_3^-$) and nitrites ($NO_2^-$) have been detected on the catalyst surface during $NO_x$ reduction and are discussed as reaction intermediates [25, 29]. For the reducing agent, partly oxidized forms of hydrocarbons as acetaldehyde and acetates have been discussed [44, 50, 63]. Moreover, organo-nitrogen species as isocyanates and cyanides have

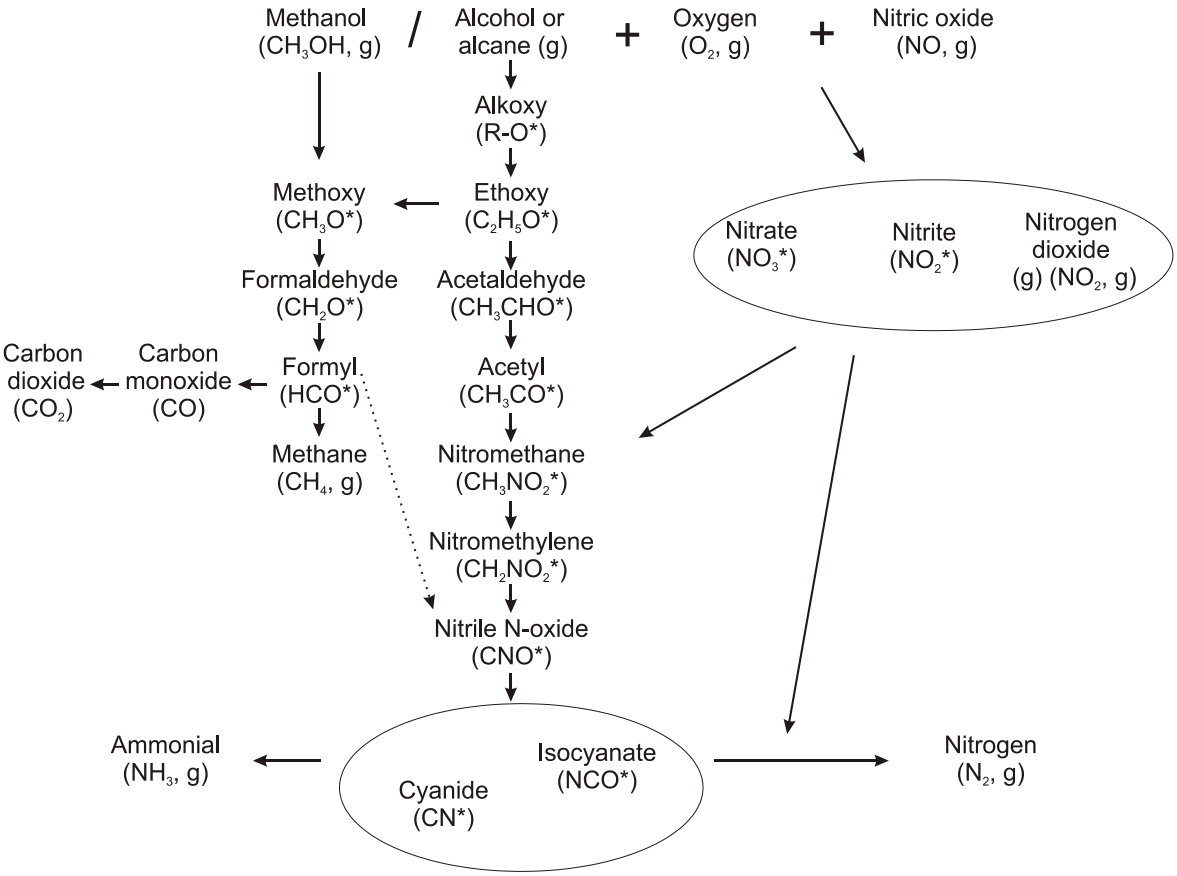


**Figure 2.2:** Proposed general reaction scheme for HC-SCR over $Ag/Al_2O_3$ adopted from Burch et al. and Mhadeshwar et al. [25, 50].

been proposed as intermediates, which can react with water forming amines and/or ammonia [44, 49, 64-66]. All of these species give $N_2$ in a reaction with $NO_x$, nitrates or nitrites. Figure 2.2 shows an example of such a reaction mechanisms over low loaded $Ag/Al_2O_3$ or $\gamma$-$Al_2O_3$ adopted from the literature [25, 50]. The formation of $N_2$ is believed to proceed via a reduced and an oxidized nitrogen species, possibly ammonia or amines and $NO_x$ or adsorbed nitrites or nitrates. These steps appear to be similar to the reactions occurring in ammonia-SCR. In this context, it has been proposed, that $N_2$ formation is the result of the decomposition of ammonium nitrite-like species [67-69]. Alternatively, the pairing of nitrogen atoms has been proposed in the earlier literature to occur via a diazonium compound (containing a N=N double-bond) [56]. However, to my knowledge such species have not been detected under $NO_x$ reduction conditions.

# 3. Experimental methods

## *3.1. Catalyst samples*

The catalyst samples, studied most extensively for DME-SCR within this work were commercial γ-$Al_2O_3$ and zeolite ZSM-5 in its acidic form. The $Al_2O_3$ catalyst powder was used as received and the ZSM-5 sample was calcined to ensure that the zeolite was in its H-form. The preparation of the silver containing samples, i.e. $Ag/Al_2O_3$ and Ag-ZSM-5 is described in detail in **papers I** and **II**, respectively. For the DRIFT experiments in **papers I** and **V**, no further processing of the powder samples was done, since they were studied in their powder form. For the flow reactor experiments in **papers I - IV**, however, the catalyst powders were washcoated on honeycomb structured cordierite monoliths. For this purpose, a slurry containing catalyst powder and binder in a weight ratio of 4:1 and water was prepared. For $Al_2O_3$ containing catalyst samples, a binder based on böhmite was used (SASOL Puralox SBa-200) and for the zeolite catalyst samples a $SiO_2$ binder (Bindzil colloidal silica 30NH3/200, Eka Chemicals). The monolith was immersed in the slurry and the channels and the outer surface of the monolith were gently blown free with air, to avoid plugging of the channels and deposition of active material on the outside of the monolith. Subsequently the monolith was dried at 90 °C and calcined at 550 °C for 2 min. These steps were repeated until the total weight of the washcoat corresponded to 20 % of the total monolith weight. Finally, the monolith was calcined in air at 550 °C for 2 h. For the transmission FTIR experiments in **paper VI**, the $Al_2O_3$ powder was washcoated on a woven wire steel mesh. Differences to the washcoating of the monoliths were that the slurry contained less water and that the desired amount of washcoat was evenly spread on the mesh in one step.

Following a heat treatment at 225 °C in vacuum, the surface area of the samples has been determined according to the BET-method by $N_2$ sorption at -196 °C using a Micromeritics ASAP 2010 instrument and found to be 355 $m^2/g$ for the H-ZSM-5 and between 176 and 200 $m^2/g$ for the $Al_2O_3$ powder, respectively.

## *3.2. Flow reactor experiments*

The flow reactor was one of the most important instruments used in this thesis and was applied with different focus in **papers I-IV**. The general set-up of the flow reactor is shown in Figure 3.1. The reactor itself consisted of an 80 cm long, horizontally mounted quartz tube, heated by a heating coil. The monolith sample was placed at the end of the tube, and the temperature was controlled in the gas stream before the catalyst and measured inside one channel in the centre of the monolith. The feed gas was mixed by a computerized multicomponent gas mixer and analysed after the catalyst by a gas phase FTIR and a $NO_x$ detector. Water was introduced through a pressurized, heated capillary and removed after the reactor by a gas dryer, since the $NO_x$ detector is sensitive to water. In **paper IV**, methanol was introduced by a liquid delivery system with vapour control, consisting of a liquid flow controller, a mass flow controller for carrier gas and a temperature controlled mixing and evaporation device.

The gas phase FTIR instrument is convenient for the analysis of gases in studies of the selective catalytic reduction of $NO_x$. Briefly, molecules with a dipole (either permanent or induced by vibration) absorb infrared (IR) radiation. The absorption is dependent on the dipole in the molecule and at the same time proportional to the concentration of this molecule. Since each type of molecule absorb specific frequencies that are characteristic for their structure, the analysis of several gases in parallel is possible. The number of detectable species is in practice limited by the overlap of the absorption bands of the species. However, a computerized analysis of the spectra in the used gas phase FTIR instrument minimizes this problem. In **paper I**, the formation of traces of gases with concentrations of less than 10 ppm has been qualitatively followed in a complex gas mixture. The main drawback of the FTIR analysis in $NO_x$ reduction experiments is that $N_2$ cannot be detected due to the absence of a dipole. The main advantage of the gas phase FTIR technique is the possibility to rapidly detect several different types of molecules at the same time

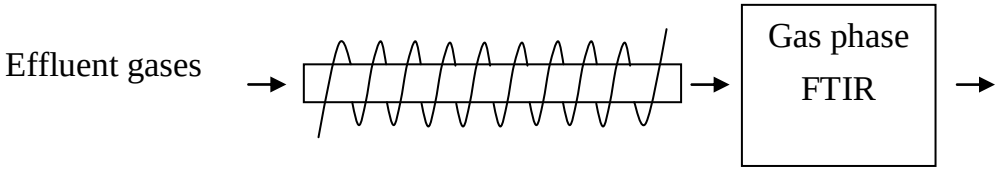


**Figure 3.1:** Scheme of the principal setup of the flow reactor.

during transients. The gas phase FTIR instrument was applied for the simultaneous detection of DME, methanol, formaldehyde, methane, CO, $CO_2$, NO, $NO_2$, $N_2O$, $NH_3$, HNCO and HCN.

In **paper III**, the characteristics of the empty reactor and the reactions occurring in the presence of DME were evaluated. Several parameters of the occurring reactions were studied. The influence of the temperature was investigated in temperature ramps, both heating and cooling ramps at 10 °C/min. Moreover, different gas mixtures containing DME, $O_2$ and $NO_x$ in varying concentrations were studied in the presence and absence of water. This experimental matrix generated a thorough knowledge of the composition of the gas mixture reaching the catalyst in the flow reactor during DME-SCR conditions.

**Papers II** and **III** comprise parameter studies, in which the activity of zeolite catalysts for $NO_x$ reduction was determined as steady state points between 200 and 500 °C in varying gas mixtures. Moreover, the impact of the counter ion on the activity for $NO_x$ reduction was studied in **paper II**. Steady state points were applied in these studies due to the high adsorption capacity of zeolites for hydrocarbons.

In **papers I** and **IV**, temperature ramps have been applied to evaluate the activity of $Al_2O_3$-based catalysts. In these studies, temperature ramps have been preferred, since they allow for continuous monitoring of the conversion of gases versus temperature. In view of the occurrence of gas phase reactions with abrupt changes in the gas composition, it was essential to capture these phenomena in the temperature ramps.

Finally, in **paper I**, step response experiments were carried out in the flow reactor, which were compared to similar experiments in the DRIFT reactor. In these experiments, NO and propene as reducing agent were sequentially added and removed from the gas mixture according to Table 3.1 and Figure 3.2 to study the catalyst performance and the gases formed under different gas mixtures and transient conditions. This type of experiments was performed for mechanistic studies. More experimental details for all the studies are given in the different papers.

| step number | gas mixture |
|---|---|
| 1 | $NO + O_2$ |
| 2 | DME or propene + $NO + O_2$ |
| 3 | DME/propene + $O_2$ |
| 4 | DME or propene + $NO + O_2$ |
| 5 | $NO + _{O2}$ |
| 6 | DME or propene + $NO + O_2$ |

**Table 3.1:** Gas mixture in the steps of the step response experiments.

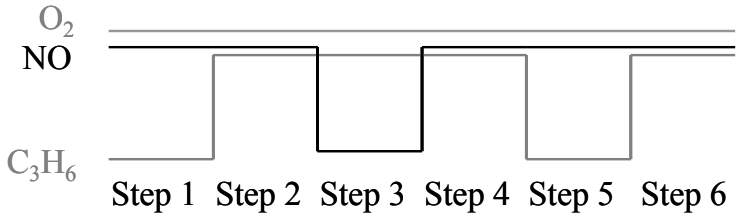


**Figure 3.2:** Illustration of the gas mixtures in a step response experiment.

## *3.3. Studies of surface species*

Surface species adsorbed on the catalyst were studied in **papers I, V** and **VI** by diffuse reflectance Fourier transformed infrared (DRIFT) spectroscopy and transmission FTIR spectroscopy. In contrast to the gas phase FTIR, the IR beam in the DRIFT cell is directed by several mirrors to the catalyst surface, where it is reflected, collected by other mirrors and analysed. In the transmission cell, the IR beam passes directly through a very thin disk of the catalyst sample. Surface species adsorbing on the catalyst surface cause IR absorption bands which can be assigned to specific species. One advantage of the applied DRIFT set-up is a very simple mounting of the sample. Moreover, the amount of the sample is large enough for catalytic conversion to be detected by a mass spectrometer. Finally, the used DRIFT cell is robust and allows for fast heating to 550 °C and cooling. Disadvantages of this cell are radial and horizontal temperature gradients in the sample volume and the inability to quantify the amount of adsorbed surface species. The DRIFT cell was applied in **papers I** and **V**. The most important advantage of the transmission cell in the context of this thesis is the exclusive heating of the sample for the study in **paper VI**. Drawbacks are the more laborious mounting and the delicate heating of the sample. Too high power in the heating causes thermal stress in the cell which

breaks the cell windows. On the other hand, when the heating power is restricted, the highest temperature which can be obtained is too low for the desired pre-treatment to be performed. More details of the transmission cell will be discussed below.

The gas composition from the DRIFT cell is analysed by a mass spectrometer. The advantage of the mass spectrometer compared to the used gas phase FTIR is the small probe volume, which allows measuring of fast changing gas compositions despite of the small flow rates applied. Moreover, the mass spectrometer itself allows for fast measurements. A major disadvantage of the mass spectrometer for DME-SCR applications is the difficulty in distinguishing between gas molecules and molecule fragments with the same mass. This fact complicates identification and quantification or makes it impossible. Molecular nitrogen ($N_2$) and CO both contribute to the mass to charge ratio m/z = 28, and $CO_2$ and $N_2O$ are both detected at m/z = 44, preventing their separate detection when no further instrument for gas analysis is available. Table 3.2 shows a selection of relevant species during DME-SCR and the masses to which they contribute. Due to the lack of masses ascribed to only one gas, the mass spectrometer was only used for qualitative measurements.

| Mass | Species |
|---|---|
| 15 | $CH_4$, $CH_3OH$, DME |
| 16 | $O_2$, $CH_4$ |
| 17 | $H_2O$, $NH_3$ |
| 18 | $H_2O$ |
| 28 | $N_2$, CO |
| 30 | NO, $NO_2$ |
| 31 | $CH_3OH$, DME |
| 32 | $O_2$, $CH_3OH$ |
| 40 | Ar |
| 44 | $CO_2$, $N_2O$ |
| 45 | DME |
| 46 | $NO_2$, DME |

**Table 3.2:** Contribution of species relevant in DME-SCR to the masses in mass spectroscopy.

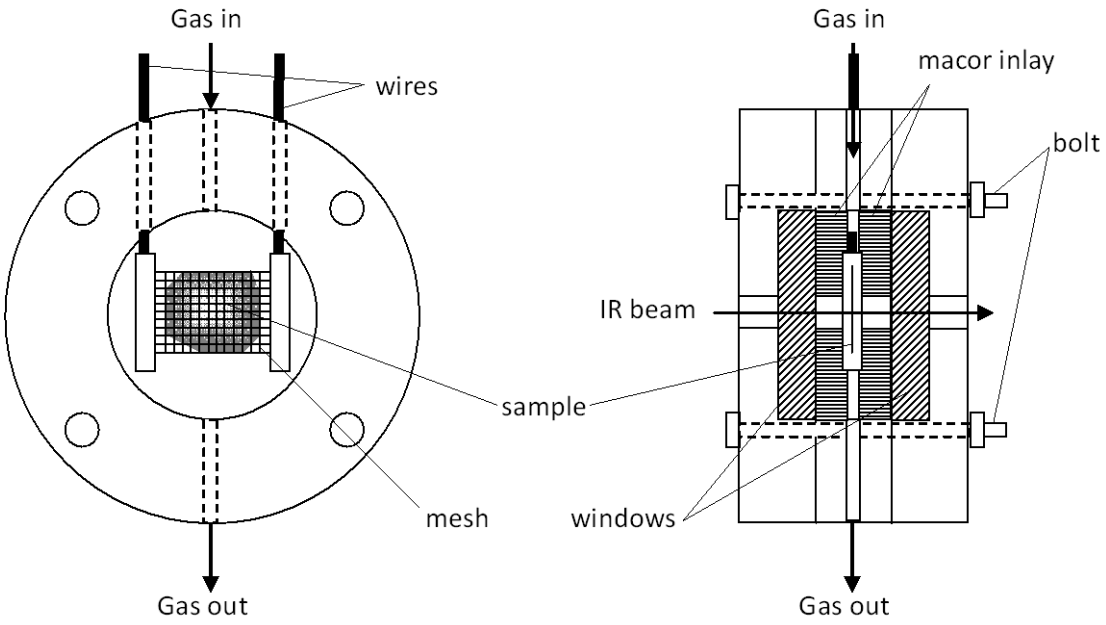


**Figure 3.3:** Schematic drawing of the home-made transmission cell. Top view and cross-section view.

In **paper VI** the objective was to study the impact of the gas phase reactions induced by DME in the presence of $O_2$ and NO on the catalyst activity. For this study, an experimental set-up was designed that allows controlling the occurrence of gas phase reactions independently of the catalyst temperature. Since these gas phase reactions occur only in a heated glass tube with sufficient residence time, such a tube was inserted into the metal tubing before the spectroscopy cell. However, in the DRIFT cell the sample is heated by a metal sample holder, which continues to oxidize the gases after they have reacted in gas phase reactions (see Chapter 4). This further oxidation excludes the use of the DRIFT cell from studies of the gas phase reactions. Instead, a home-made transmission cell was applied, whose set-up is illustrated in Figure 3.3. In this cell, the catalyst is placed on a woven wire steel mesh, which is heated by resistive heating. Since the mesh is coated by the catalyst sample, the oxidation of the species formed in the gas phase reaction on hot metal surfaces is minimized and, moreover, only the catalyst support is actively heated and not the gases. A major problem with the transmission cell is, however, that the sample acts as an IR source. This radiation increases with increasing temperature especially in the region of wavenumbers between 1000 and

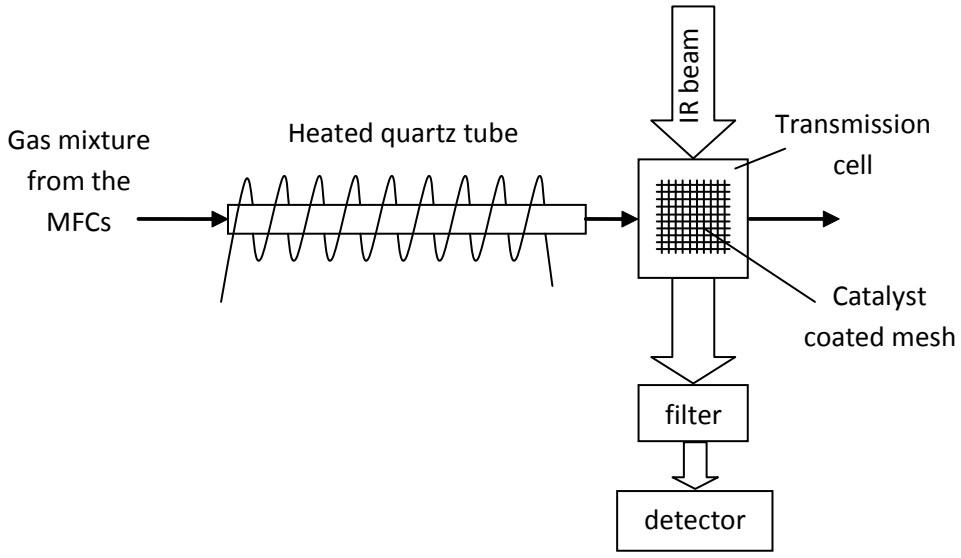


**Figure 3.4:** Schematic drawing of the experimental set up used to independently control catalyst temperature and occurrence of gas phase reactions used in the experiments with the transmission cell.

2000 $cm^{-1}$.Therefore the IR radiation of the sample hinders collection of spectra in this region above 250 °C. Consequently a quartz glass filter was placed in front of the IR detector in all experiments conducted at 350 °C. To collect spectra in the wavenumber region from 1150 to 4000 $cm^{-1}$ without the filter the cell was intermittently cooled to 250 °C in Ar. The experimental set-up with filter is schematically shown in Figure 3.4.

Surface species have been studied in **papers I, V** and **VI**. In **paper I**, NO and propene were switched on and off in a step response experiment according to Table 3.1, while the formation and consumption of surface species was monitored and correlated to gas species obtained in similar flow reactor experiments. The correlation of surface species to gas species observed in step response experiments is a powerful tool to investigate reaction mechanisms.

**Papers V** and **VI** are closely connected to each other. Since very little is published on $NO_x$ reduction with DME, the temperature programmed desorption experiments in **paper V** served to gain insight in to this system. These types of experiments facilitate the allocation of absorption bands to surface species thanks to the limited number of possible species when only DME or $NO_x$ had been adsorbed on the sample. Moreover, the occurrence of gas phase reactions needs not be considered

with this set-up, since DME is adsorbed at 30 °C, where no reactions occur in the gas phase.

Finally, in **paper VI,** the effect of the gas phase reactions on the selective catalytic reduction of NO with DME was studied. For this purpose, the experimental set-up needed to be adjusted considerably, as discussed before. The main advantages with the applied set-up are that the occurrence of the gas phase reactions can be controlled independently of the catalyst temperature and that the formation of surface species can be studied while gas phase reactions occurred before the catalyst sample. It had been desirable to correlate the surface species to species formed in the gas phase similar to **paper I**. However, in the flow reactor, the catalyst and the gases are heated by the same heating coil and therefore, the occurrence of gas phase reactions is implicitly coupled to the catalyst temperature. The step-response experiments, thus, cannot be performed under comparable conditions in the flow reactor preventing a correlation of surface species to results from the flow reactor. Moreover, the flow rates in the transmission cell are too small for transient behaviour to be measured in the gas phase FTIR cells available to us. Therefore, only the $NO_x$ conversion at 250 and 350 °C was determined in the presence and absence of gas phase reactions in steady state points.

# 4. Gas phase reactions during DME-SCR

In the catalytic reduction of $NO_x$ with hydrocarbons, the reactants are regarded kinetically stable and reactions are expected to be limited in an empty flow reactor in lab scale at temperatures typical for HC-SCR. Therefore, tests with the empty reactor serve mainly to check reactor parameters as for example residence times and mixing characteristics. However, considerable amounts of DME react in the presence of oxygen in the empty reactor as shown in Figure 4.1. At the same time, CO, formic acid and formaldehyde are detected as main products, but only minor amounts of $CO_2$. Another uncommon feature in the SCR context is that DME conversion reaches a local maximum at about 320 °C before decreasing again. This maximum in DME conversion results in maxima in the CO and formic acid yields at about the same temperature and does not depend on the absolute DME concentration for the two concentrations studied. Furthermore, the shapes of the concentration curves versus temperature are similar during heating and cooling ramps. In areas outside $NO_x$ reduction applications, these characteristics of DME

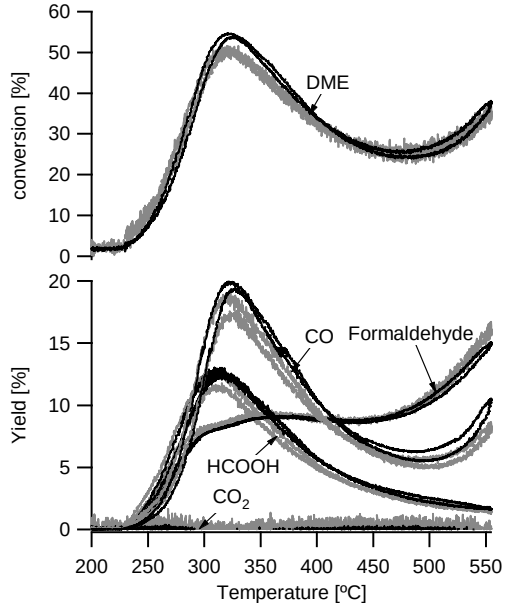


**Figure 4.1**: DME conversion through radical reactions between DME and $O_2$ as a function of temperature in an empty quartz glass tube with two different DME concentrations, in a gas mixture of 8% $O_2$ and 250 ppm DME (grey) or 1000 ppm DME (black) balanced in Ar. Both heating and cooling ramps at 10 °C/min are included.

mixtures are well known e.g. for the ignition of DME in an engine and similar oxidation curves have earlier been reported in the literature [70-72]. In these applications, the observed DME oxidation has been explained by radical reactions, typical for low-temperature ignition of hydrocarbons [70, 72-74]. According to these studies, the conversion of DME is initiated by a reaction where a DME molecule splits into an $H_3CO^{\bullet}$ radical and a $CH_3^{\bullet}$ radical (4.1).

$$H_3C\text{-}O\text{-}CH_3 \rightarrow H_3CO^{\bullet} + CH_3^{\bullet} \quad (4.1)$$

In a following complex scheme of radical reactions, $OH^{\bullet}$ radicals are formed, which in turn initiate the oxidation of other DME molecules by abstraction of a hydrogen atom forming a methoxymethyl radical ($H_3C–O–CH_2^{\bullet}$) according to reaction 4.2 [70, 73, 75].

$$H_3C\text{-}O\text{-}CH_3 + OH^{\bullet} \rightarrow H_3C\text{-}O\text{-}CH_2^{\bullet} + H_2O \quad (4.2)$$

These methoxymethyl radicals have been shown to react with $O_2$ giving the peroxy radical $H_3C\text{-}O\text{-}CH_2OO^{\bullet}$ (reaction 4.3), which has been proposed to be an important intermediate in the oxidation of DME [74].

$$H_3C\text{-}O\text{-}CH_2^{\bullet} + O_2 \rightarrow H_3C\text{-}O\text{-}CH_2OO^{\bullet} \quad (4.3)$$

Moreover, the formation of formaldehyde and formic acid as well as the existence of a local maximum in DME conversion has been described in a detailed model by Dagaut et al. [76] and has been discussed in **paper III**.

In the presence of NO, the characteristics of the DME oxidation differ significantly from those discussed before. The addition of NO to the gas mixture of DME and $O_2$ inhibits the oxidation of DME below 300 °C, and enhances the oxidation above 400 °C for all studied DME/NO ratios. Moreover, above 300 °C the conversion of DME sharply increases to over 70 % conversion in a temperature interval of less than 20 °C for DME/NO ratios of 2 and 4 as shown in Figure 4.2. At lower DME/NO ratios, the increase in the conversion of DME is shifted to higher temperatures and becomes less sharp. At the same temperature, where DME is converted, CO, formaldehyde and formic acid are formed. Simultaneously, NO is almost completely oxidized to $NO_2$ at DME/NO ratios higher than 2. At lower DME/NO ratios, the oxidation of NO to $NO_2$ is shifted to higher temperatures, is

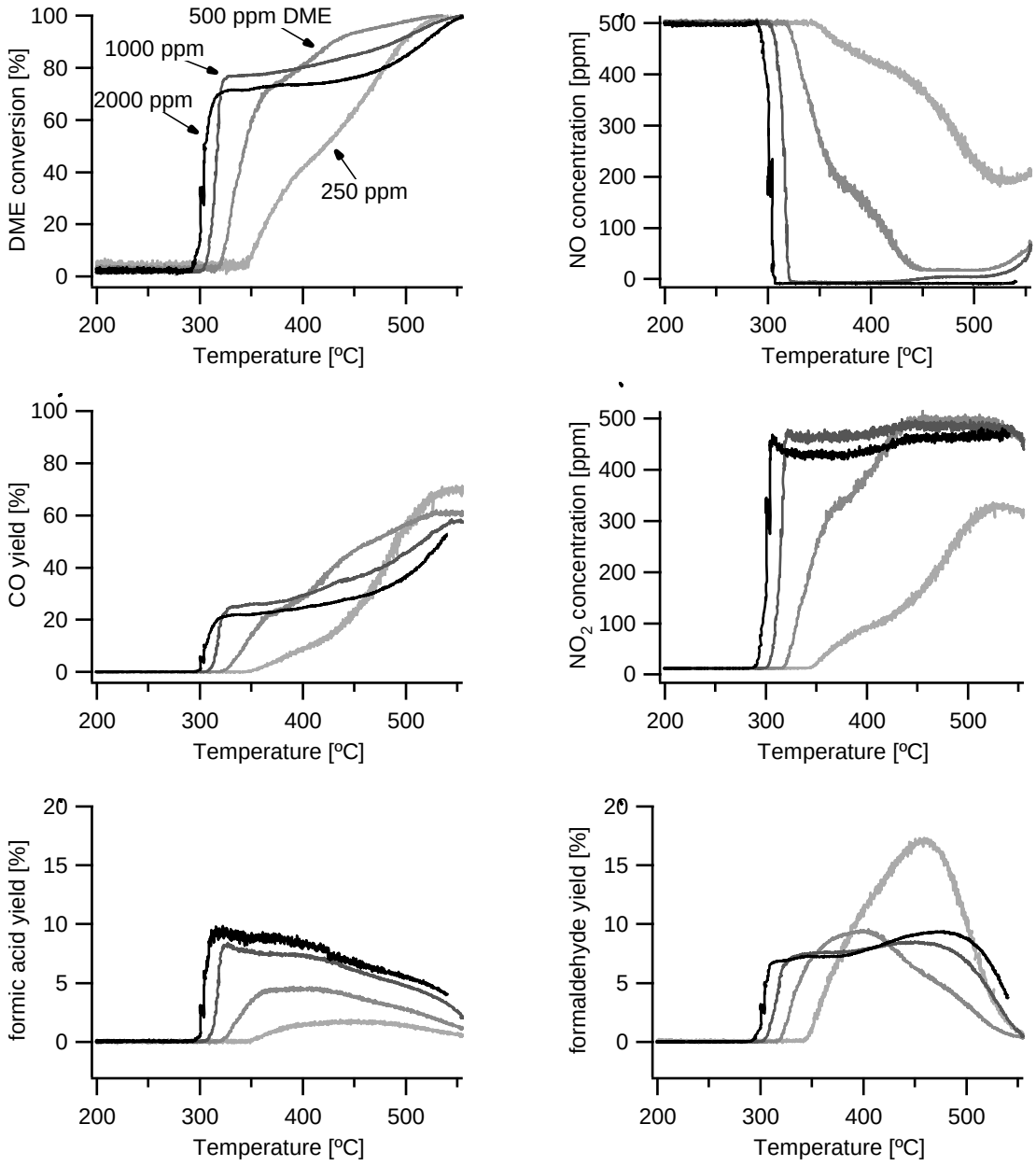


**Figure 4.2:** DME conversion, NO and $NO_2$ concentrations and yields of CO, formic acid and formaldehyde during gas phase reactions with DME, NO and $O_2$ as function of temperature during a heating ramp with different DME concentrations, in a gas mixture of 500 ppm NO, 8% $O_2$ and 250 ppm DME (light grey), 500 ppm DME (darker grey), 1000 ppm DME (dark grey) or 2000 ppm DME (black) balanced in Ar.

not complete within the studied temperature range, and increases not as sharply. Bearing in mind the equilibrium reaction of the direct oxidation of NO with $O_2$ to $NO_2$ (reaction 4.4),

$$2\ NO + O_2 \leftrightarrow 2\ NO_2 \quad (4.4)$$

the formation of high amounts of $NO_2$ is unexpected, since it is significantly higher than allowed by the thermodynamic restrictions of this reaction as illustrated in Figure 4.3.

It is thus obvious that $NO_2$ is formed through another pathway. In the literature it has been reported that $NO_2$ may form by the reaction of the previously named peroxy-radical $H_3C\text{-}O\text{-}CH_2OO^{\bullet}$ and $NO^{\bullet}$, according to reaction 4.5 [76, 77].

$$H_3C\text{-}O\text{-}CH_2OO^{\bullet} + NO^{\bullet} \rightarrow CH_3OCH_2O^{\bullet} + NO_2^{\bullet} \quad (4.5)$$

The formation of $NO_2$ from the reaction of NO with a peroxy-radical seems to be more general since formation of high amounts of $NO_2$ with propane and propene in an empty reactor above 500 °C has been explained by reaction 4.6 [78].

$$NO^{\bullet} + HO_2^{\bullet} \leftrightarrow NO_2^{\bullet} + OH^{\bullet} \quad (4.6)$$

Besides these explanations from the literature, we speculate in **paper III** that the inhibition in DME oxidation in the presence of NO is due to recombination reactions between recently formed $CH_3^{\bullet}$ or $OCH_3^{\bullet}$ radicals and $NO_x$ (4.7 and 4.8).

$$CH_3^{\bullet} + NO_x^{\bullet} \rightarrow CH_3\text{-}NO_x \quad (4.7)$$

$$OCH_3^{\bullet} + NO_x^{\bullet} \rightarrow H_2CO + HNO_x \quad (4.8)$$

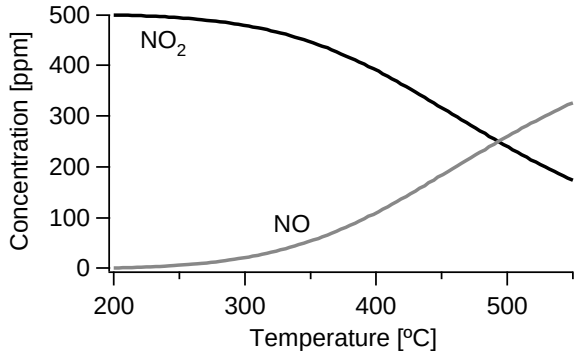


**Figure 4.3:** Equilibrium concentrations for the reaction of NO and $O_2$ to $NO_2$ for 500 ppm $NO_x$ and 8 % $O_2$ calculated not allowing formation of $N_2$ with the HSC Chemistry software [79].

More details of the gas phase radical reactions occurring in the empty glass tube have been discussed in **paper III**. However, the insight into the gas phase reaction, which has been provided, allows discussing and explaining the special characteristics of DME-SCR.

# 5. Catalysts for DME-SCR

Catalysts that have been applied for DME-SCR in the literature can be divided into two groups: zeolite based catalysts, i.e. Cu-ZSM-5, Ag/ZSM-5 and Ag/mordenite, and $Al_2O_3$ based catalysts, i.e. $Ag/Al_2O_3$, $V_2O_5/Al_2O_3$, $Ga_2O_3/Al_2O_3$, $Mo/Al_2O_3$, $Sn/Al_2O_3$ and $Co/Al_2O_3$ as described in chapter 2.1 [21, 30, 36-38]. For the present thesis, H-ZSM-5 and $\gamma$-$Al_2O_3$ have been studied in greatest detail. The H-ZSM-5 catalyst has also been ion-exchanged with several counter ions and the activity for $NO_x$ reduction has been determined. Parts of these results have been presented in **paper II** and will be discussed in chapter 5.1. The $\gamma$-$Al_2O_3$ catalyst has been compared to a $Ag/Al_2O_3$ catalyst, and a comparison with methanol has been conducted in **papers IV** and **V** and will be briefly discussed in chapter 5.2.

## *5.1. Zeolite based catalysts for DME-SCR*

Acidic ZSM-5 (H-ZSM-5) samples have been studied for DME-SCR in **papers II** and **III**. Figure 5.1 shows that $NO_x$ is reduced in considerable amounts above 300 °C and the activity for $NO_x$ reduction increases with temperature reaching 20 % at 500 °C in the absence of water. At these temperatures, where $NO_x$ reduction occurs, DME is oxidized and CO and $CO_2$ are formed. Adding water to the system increases $NO_x$ reduction at 350 °C but decreases it above 400 °C as shown in Figure 5.1. Moreover, DME conversion starts at lower temperatures due to DME conversion to methanol. Formaldehyde is a by-product during DME-SCR over H-ZSM-5. Increasing the amount of reducing agent increases the $NO_x$ reduction reaching a maximum of 28 % $NO_x$ reduction at 450 °C for a DME/NO ratio of 4 (1900 ppm DME, 475 ppm NO). The achieved $NO_x$ conversion is clearly lower than the best conversions reported in the literature. However, activity is generally lower over coated monolith catalysts than over powder catalysts with comparable space velocity due to less active material per volume in a monolith catalyst compared to a powder bed. Moreover, the presence of water decreases $NO_x$ conversion, which further complicates the comparison between some literature data and the results presented herein.

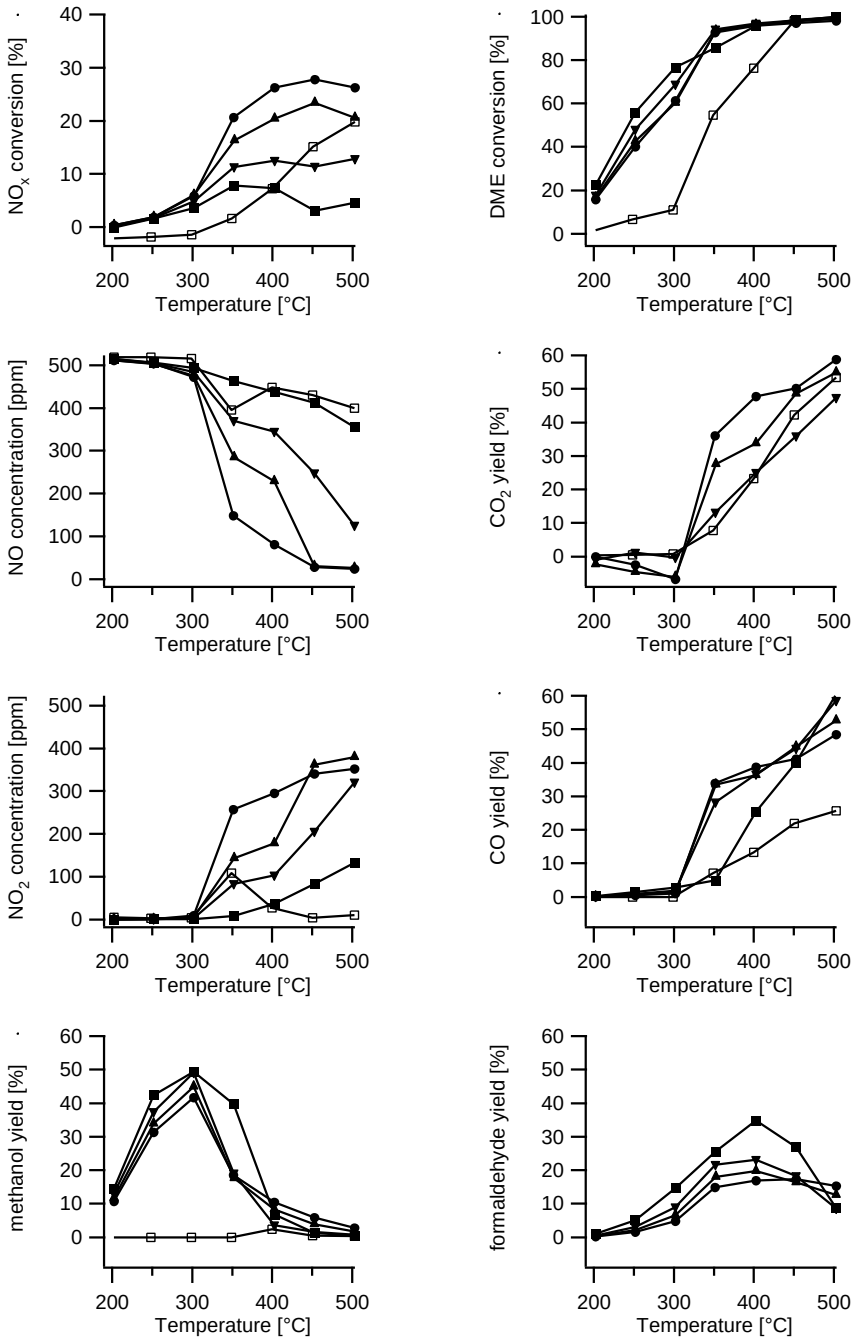


**Figure 5.1:** Conversion, yield and concentration of gases during DME-SCR of NO over H-ZSM-5 as a function of temperature in the absence of water (□) and in the presence of 5 % water (filled symbols). Gas mixture: 1000 ppm NO, 8 % $O_2$ and 1000 ppm DME (□), and 475 ppm NO, 7.6% $O_2$, 5 % $H_2O$ and 475 ppm DME (■), 950 ppm DME (▼), 1425 ppm DME (▲) and 1900 ppm DME (●).

Another parameter that has been evaluated is the acidity of the H-ZSM-5 sample. Zeolites as ZSM-5 are highly structured materials made of silicon atoms tetrahedrally bound to four oxygen atoms. These silicon atoms may be replaced by aluminium atoms in the structure. Since the valence number of aluminium (three) is less than that of silicon (four) a negative charge is introduced into the structure, which needs to be compensated by a counter cat-ion. When protons act as cat-ions they form acidic sites. Thus, the total acidity (amount of acid sites) of the ZSM-5 zeolite increases with the amount of aluminium atoms replacing silicon. In a series of ZSM-5 samples with silicon to aluminium molar ratios (Si/Al) of 1026, 476, 170, 80 and 54, the sample with the Si/Al ratio of 80 was found to be most active for $NO_x$ reduction with DME. In previous studies it had been shown that the activity for $NO_x$ reduction increased with the acidity of γ-alumina and ZSM-5 catalysts [30, 80] and it has been suggested that the acidic sites are involved in $NO_x$ reduction [80] to explain this observation. However, since ZSM-5 is also used as cracking catalysts in the petroleum industry and in the methanol-to-olefin (MTO) process [81-83], ZSM-5 zeolites with very high acidity are prone to coking, suggesting a optimum in acidity for $NO_x$ reduction. Therefore, if not stated otherwise, all the experiments with ZSM-5 were carried out over the Si/Al = 80 sample.

For $Ag/Al_2O_3$ in conventional HC-SCR it has been reported that reactions occur also in the gas phase, indicated by a drop in $NO_x$ reduction activity when an oxidation catalyst was placed directly behind the $Ag/Al_2O_3$ catalyst [84]. This behaviour has been explained by gas phase reactions occurring behind the catalyst

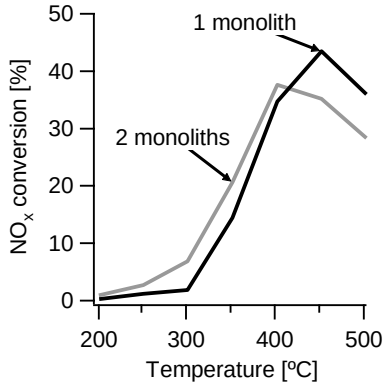


**Figure 5.2:** Influence of the geometry of the monolith, using one or two similar monoliths and adjusting the gas flow containing 500 ppm NO, 2000 ppm DME, 8 % $O_2$ and 5 % $H_2O$ in Ar to a space velocity of 16 700 $h^{-1}$.

[45, 84]. Since gas phase reactions are only rarely reported for $NO_x$ reducing conditions in general and gas phase reactions occur in DME-SCR, experiments were carried out to examine whether the geometry, i.e. the ratio of length to diameter of the catalyst at a constant space velocity has a significant influence also for the present system. Therefore, two similar H-ZSM-5 monoliths were placed with a gap of 2 cm between them in the flow reactor and the activity for $NO_x$ reduction was measured as a function of temperature shown in Figure 5.2. The same experiment was repeated with only one monolith and half of the gas flow to maintain a constant space velocity. As illustrated in Figure 5.2, the geometry of the monolith had no clear impact on the $NO_x$ conversion under the applied conditions. However, due to the lower space velocity compared to Figure 5.1, the maximum in $NO_x$ conversion is higher reaching 43 % and 38 % when using one or two monoliths, respectively.

Masuda et al. tested silver-zeolite catalysts in real exhaust gas from a diesel engine and suggested that silver mordenite is suitable for $NO_x$ reduction with DME [36]. To verify these results, the H-ZSM-5 catalyst was partly ion-exchanged with silver. However, the activity for $NO_x$ reduction over the Ag/H-ZSM-5 catalyst showed a maximum in $NO_x$ conversion of 10 %, which is considerably lower than over the acidic H-ZSM-5 as shown in Figure 5.3. Another ZSM-5 sample containing both Ag and trace amounts of Na as counter ions, showed comparable activity for $NO_x$ conversion but the oxidizing activity is higher and the selectivity towards partially oxidized carbon containing products is lower as reported in more detail in **paper II.**

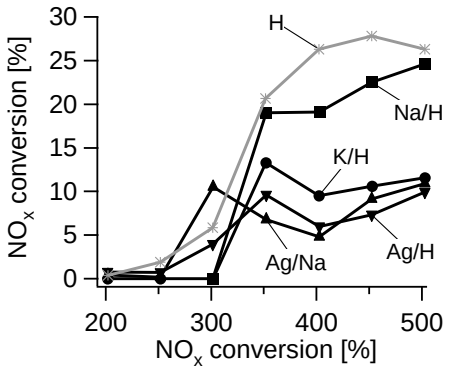


**Figure 5.3:** $NO_x$ conversion during DME-SCR of NO over Ag/H-ZSM-5 (▼), Ag/Na-ZSM-5 (▲) Na/H-ZSM-5 (■), K/H-ZSM-5 (●) and H-ZSM-5 (Ж) as a function of temperature. Gas mixture 475 ppm DME, 475 ppm NO, 7.6 % $O_2$ and 5 % $H_2O$ in Ar.

| Sample | atom ratio Ag/Al | atom ratio Na/Al | atom ratio K/Al |
|---|---|---|---|
| H-ZSM-5 | - | - | - |
| Ag/H-ZSM-5 | 0.61 | - | - |
| Ag/Na-ZSM-5 | 0.80 | 0 | - |
| Na/H-ZSM-5 | - | 0.43 | - |
| K/H-ZSM-5 | - | - | 0.30 |

**Table 5.1:** Ratios of counter cat-ions to aluminium atoms in the zeolite structure in the ZSM-5 samples as determined by SEM-EDX.

In that paper we concluded, that the Brønsted acidic sites of the acidic ZSM-5 are crucial for $NO_x$ reduction over ZSM-5 based catalysts. In later experiments Na/H-ZSM-5 and K/H-ZSM-5 samples showed maxima in $NO_x$ conversion of 25 and 13 %, respectively as shown in Figure 5.3. These results stress, that the poorer activity for $NO_x$ reduction of the silver containing ZSM-5 samples is not only caused by the lack of Brønsted acid sites. The type of counter ion is also of importance. As presented in Table 5.1, the potassium containing sample contains less ions other than H but is not the sample with the highest activity. However, the activity for $NO_x$ reduction is lower over all ion-exchanged samples compared to over the H-ZSM-5 catalyst.

## *5.2. Activity for $NO_x$ reduction with DME over γ-alumina*

Catalyst samples based on γ-alumina are another type of samples examined for DME-SCR in this thesis and they have been applied in **papers IV-VI**. Figure 5.4a, taken from **paper IV**, shows the activity for $NO_x$ reduction over the γ-$Al_2O_3$ catalyst. Conversion of $NO_x$ is observed between 300 and 550 °C with a maximum of 47 % at 380 °C. The selectivity towards $N_2$ is presumed to be high, since only trace amounts of other N-containing species than $NO_x$, such as $N_2O$, are observed. Similar to the experiments over H-ZSM-5, $NO_x$ reduction starts at the same temperature as DME conversion, while $NO_2$, $CO_2$, CO, methanol, formic acid and formaldehyde are formed. Comparing $NO_x$ reduction over H-ZSM-5 in Figure 5.1 with that over $Al_2O_3$ in Figure 5.4a stresses the similarities between the two catalysts. However, a detailed comparison is not possible, due to different amounts of NO in the two experiments in the absence of water, or, at identical NO and DME concentrations, water is present in the experiments over H-ZSM-5 (Figure 5.1) but not in the experiments over $Al_2O_3$ (Figure 5.4a).

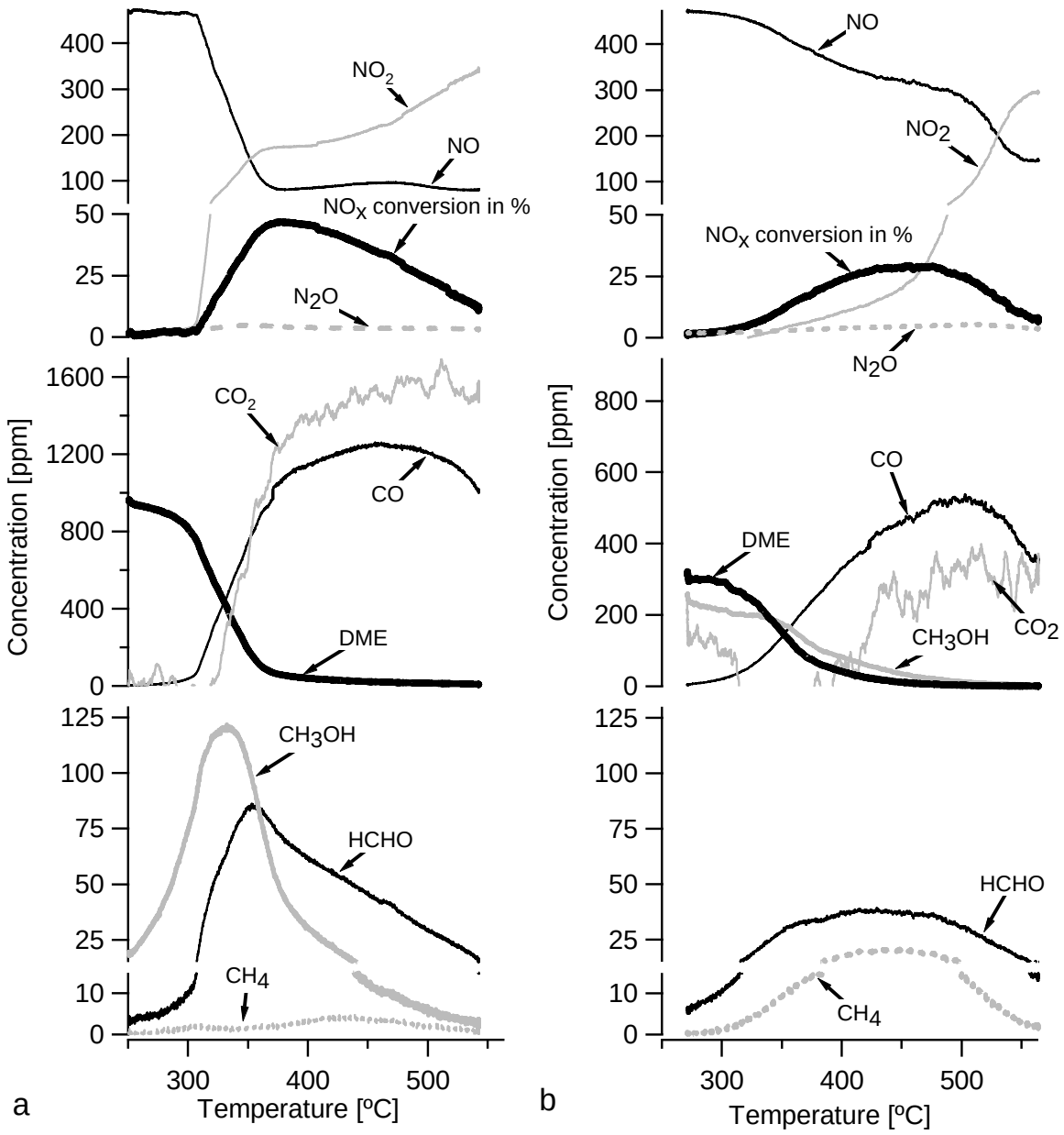


**Figure 5.4:** Catalytic activity tests over a γ-$Al_2O_3$ catalyst as a temperature ramp from 550 to 250 °C in a gas mixture of 1000 ppm DME (a) or 1000 ppm methanol (b), 500 ppm NO and 8 % $O_2$ balanced in Ar.

Methanol is formed in considerable amounts during DME-SCR over γ-$Al_2O_3$ as well as over H-ZSM-5 in the presence of water as shown in Figure 5.1 and Figure 5.4, respectively. Methanol formation is expected, since DME is produced from methanol over $Al_2O_3$ catalysts as already discussed in chapter 1.1 [6, 85-87]. Methanol-SCR was carried out over $Al_2O_3$ to further examine the similarities

between DME and methanol as reducing agents and the results are presented in Figure 5.4b. With methanol as reducing agent, $NO_x$ was reduced between 300 and 550 °C with high selectivity to $N_2$, as indicated by the low formation of $N_2O$. In the same temperature range $CO_2$, CO and formaldehyde were detected, and, in contrast to DME-SCR, methane. Moreover, below 350 °C, up to 2/3 of the methanol was converted to DME. Despite the high DME concentration, no gas phase reactions are observed below 500 °C where the $NO_2$/NO ratio is less than unity. Apparently, the retention time in the reactor after the catalyst is too short to allow for the ignition of gas phase reactions with the formed DME. Further, no gas phase reactions have been observed below 500 °C in empty reactor experiments with methanol (not shown). Conversion of $NO_x$ is considerably lower during $NO_x$ reduction with 1000 ppm methanol than with 1000 ppm DME between 300 and 350 °C but similar above 400 °C over a $\gamma$-$Al_2O_3$ catalyst and similar between 250 and 500 °C over a $Ag/Al_2O_3$ catalyst. Moreover, the increase in $NO_x$ conversion above 300 °C is less steep with methanol than with DME over $\gamma$-$Al_2O_3$. In **paper IV**, it was therefore concluded that the activity for $NO_x$ reduction with DME could be explained by the activity for $NO_x$ reduction with methanol under conditions, when the gas phase reactions are not the crucial factor. The effect of the gas phase reactions on DME-SCR will be discussed in more detail in chapter 5.3.

## *5.3. Effect of the gas phase reactions and the catalyst on the reduction of $NO_x$*

In Figure 5.5 and in **paper III**, the separate influence of the gas phase reactions and the catalyst on the gas conversion is investigated over $\gamma$-$Al_2O_3$ or H-ZSM-5 catalysts, respectively. The reduction of $NO_x$ starts at the same temperature as the gas phase reactions, but a catalyst is needed for distinct reduction of $NO_x$ with high selectivity to $N_2$, since the $NO_x$ conversion observed in the empty reactor was ascribed to the formation of nitric acid ($HNO_3$). However, the amount of formed nitric acid could not be quantified with the used gas phase FTIR instrument due to deposition of nitric acid on the windows of the instrument. Other effects of the catalysts are the formation of $CO_2$ under $NO_x$ reducing conditions and the formation of methanol at temperatures, where the catalysts are not active for $NO_x$ reduction. In the empty reactor, no methanol has been observed. Moreover, no acid, i.e. formic acid or nitric acid are detected in the presence of a catalyst, in contrast to

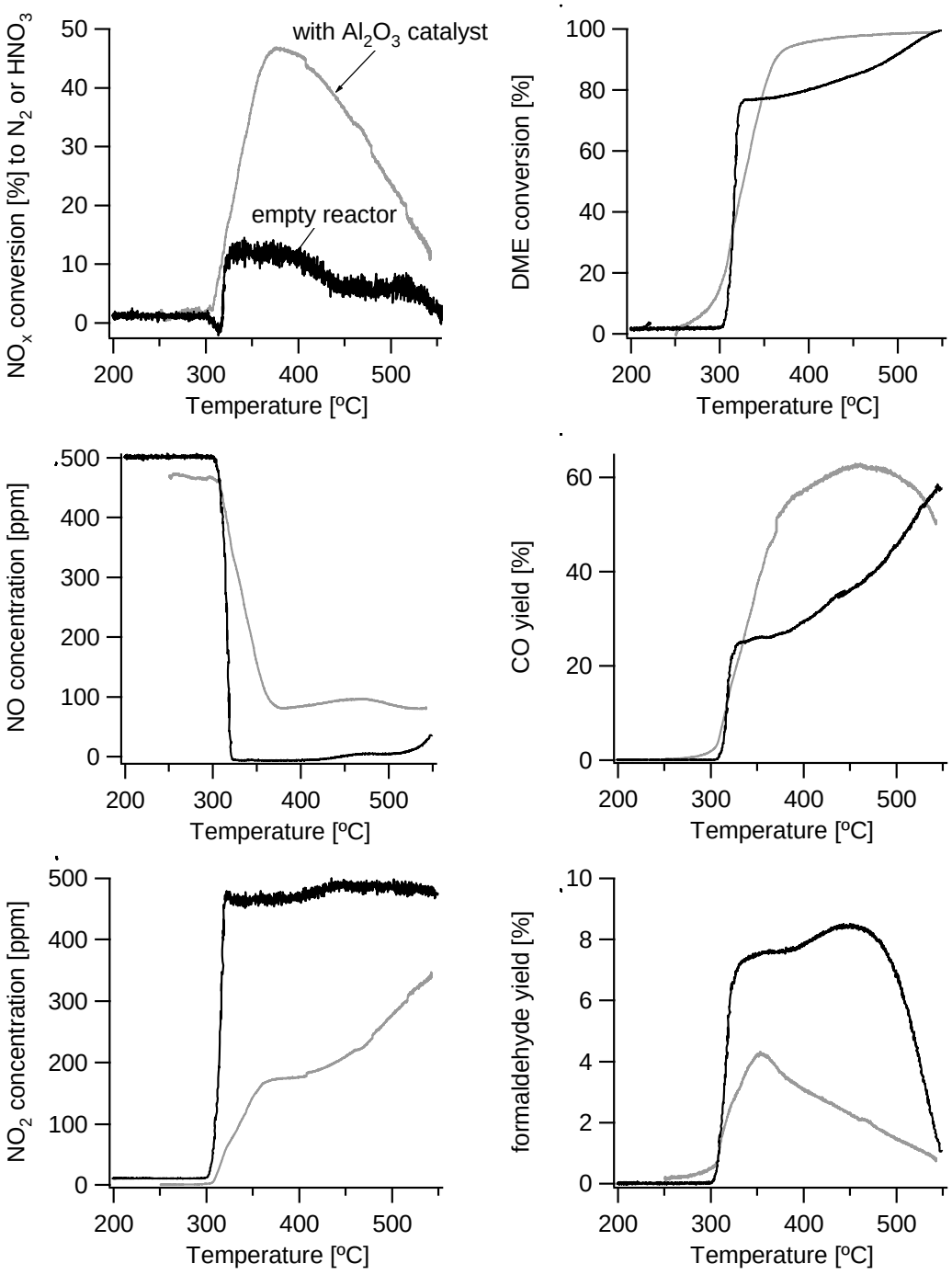


**Figure 5.5:** Comparison of gas composition between gas phase reactions (black line, heating ramp) and an $Al_2O_3$ catalyst (grey line, cooling ramp) as function of temperature in a gas mixture of 1000 ppm DME, 500 ppm NO and 8 % $O_2$ balanced in Ar. $NO_x$ conversion with catalyst shows high selectivity to $N_2$, whereas without catalyst the selectivity is high to $HNO_3$.

experiments with the empty reactor. For CO and formaldehyde, the impact of the two catalysts is different. The $Al_2O_3$ catalyst decreases the formaldehyde

concentration but increases the CO concentration as illustrated in Figure 5.5, while the H-ZSM-5 catalyst increases the formaldehyde concentration and has virtually no impact on the CO concentration.

As mentioned in the previous paragraph, the reduction of $NO_x$ occurs over both the H-ZSM-5 and the $Al_2O_3$ catalyst only at temperatures, where gas phase reactions occur. This indicates a major impact of the gas phase reactions on the catalyst activity for $NO_x$ reduction. In the flow reactor the catalyst and the gases are simultaneously heated by the same heating coil around the glass tube as illustrated in Figure 3.1, preventing a separate control of the catalyst temperature and the gas phase reactions. Therefore, an experimental set-up was assembled which allows for an independent control of the catalyst temperature and the occurrence of gas phase reactions as described in more detail in chapter 3.3 and illustrated in Figure 3.4. A limitation of this system for the analysis of the gas composition was the small gas flow of 50 ml/min through the transmission cell in connection with a gas cell of 500 ml in the gas phase FTIR instrument, leading to long stabilisation times for the concentrations in the gas cell. However, the $NO_x$ conversion was measured in steady state conditions over the $Al_2O_3$ sample at 250 °C, which is well below the onset of the gas phase reactions in the flow reactor, and at 350 °C, where gas phase reactions take place in the flow reactor. Moreover, at 350 °C the activity for $NO_x$ reduction is high over the $\gamma$-$Al_2O_3$ catalyst in the flow reactor.

At 250 °C, the activity for $NO_x$ reduction with DME over a $\gamma$-$Al_2O_3$ catalyst was found to be higher in the presence of gas phase reactions, in contrast to 350 °C where the $NO_x$ conversion is lower when gas phase reactions occur, as summarized in Table 5.2. In **paper VI**, the contradictory effect of the gas phase reactions for

| catalyst temperature | 250 °C | 350 °C |
|---|---|---|
| $NO_x$ conversion in the absence of gas phase reactions | 19 % | 58 % |
| $NO_x$ conversion in the presence of gas phase reactions | 31 % | 46 % |

**Table 5.2:** $NO_x$ conversion at a catalyst temperature of 250 °C and 350 °C, depending on the occurrence of gas phase reactions before the catalyst, in a gas mixture of 1000 ppm DME, 500 ppm NO and 8 % $O_2$ in Ar.

$NO_x$ reduction activity was explained for 350 °C by a simplified view of the gas phase reactions as a partial oxidation of DME. At this catalyst temperature, $NO_x$ reduction decreases with decreasing DME concentration as shown in Figure 5.1. Thus, the consumption of DME in gas phase reactions results in diminished $NO_x$ reduction at a catalyst temperature of 350 °C. On the other hand, $NO_x$ conversion was shown to be higher with $NO_2$ than with NO in synthetic exhaust gas mixtures over $\gamma$-$Al_2O_3$ catalysts [29, 31]. Apparently, the positive effect of the formation of $NO_2$ in the gas phase reactions prevails at 250 °C. This view is also supported by transmission FTIR-data as will be discussed in chapter 6.2.

The observed $NO_x$ conversions in the transmission cell (Table 5.2) are higher than those observed in the flow reactor (Figure 5.4) at 250 °C in the absence of gas phase reactions and at 350 °C in the presence of gas phase reactions. This difference may be explained by different reactor systems with different types of catalyst heating and different space velocities.

# 6. Mechanistic aspects of DME-SCR

In order to develop catalysts for a specific application, the system needs to be well characterised. One of the parameters characterizing a system for the catalytic reduction of $NO_x$ is the reaction mechanism. As previously discussed in chapter 2.3, the reaction mechanism depends on the reducing agent and the catalyst. In the following, the reaction mechanism for DME-SCR over a $\gamma$-$Al_2O_3$ catalyst will be presented. Since the reaction mechanism cannot be studied directly, the accumulation and consumption of surface species was studied by FTIR. In **paper V**, a basic understanding of the processes was achieved through several temperature programmed desorption and reaction experiments in a diffuse reflectance Fourier transform infrared (DRIFT) spectroscopy cell at the same time as the gas composition was analysed by a mass spectrometer. These experiments facilitate assignment of the observed bands due to a limited number of involved species in the individual experiments as discussed in chapter 6.1. For convenient reading, the assignment of the bands with references to the literature is summarized in Table 6.1 and not discussed in detail in the text. Based on this knowledge mechanistic aspects of DME-SCR over $\gamma$-$Al_2O_3$ are discussed in chapter 6.2 and will be compared to results obtained for propene-SCR over $Ag/Al_2O_3$ in chapter 6.3. Finally, a reaction mechanism for DME-SCR over $\gamma$-$Al_2O_3$ will be proposed in chapter 6.4.

| Wavenumber [$cm^{-1}$] | Surface species | References |
|---|---|---|
| 3792 | hydroxyl | [88-90] |
| 3772 | hydroxyl | [88-90] |
| 3735 | hydroxyl | [88-90] |
| 3684 | hydroxyl | [88, 90] |
| 3200 | methanol | [40, 90] |
| 3031 | methoxy | [91] |
| 3001 | formate | [29, 63, 92] |
| 2960-2955 | methoxy | [90, 91] |
| 2946-2941 | methoxy or methanol | [90, 93] |
| 2928 | DME | [91], **paper VI** |
| 2909 | formate | [63, 92, 94] |
| 2881 | methoxy | [91] |

| Wavenumber [$cm^{-1}$] | Surface species | References |
|---|---|---|
| 2851-2842 | methoxy | [40, 86, 90, 91] |
| 2821 | methoxy or methanol | [90, 93] |
| 2808 | formaldehyde like | **paper V** |
| 2257 | NCO | [95] |
| 2234 | NCO | [95, 96] |
| 2167 | CN | [95, 97-99] |
| 1630-1570 | nitrates and nitrites | [34, 51, 63, 92, 99, 100] |
| 1595-1590 | formate | [63, 87, 92, 94, 99] |
| 1556-1549 | nitrate | [34, 97, 99-101] |
| 1531 | formohydroxamic acid (CHO-N(H)OH) | [34, 102], **paper V** |
| 1474 | methoxy | [39, 90, 91] |
| 1460-1455 | methoxy | [39, 90, 91] |
| 1393 | formate | [44, 63, 87, 92, 94, 98, 99, 103] |
| 1377 | formate | [44, 63, 87, 92, 94, 98, 99, 103] |
| 1325 | nitrite | [29, 97, 104] |
| 1300-1304 | nitrate | [94, 97, 99, 100, 105, 106] |
| 1260 | methoxy | [91] |
| 1246 | nitrate | [97, 99, 100] |
| 1234 | nitrite | [29, 97] |
| 1192 | methoxy | [40, 86] |
| 1160 | methoxy | [91] |

**Table 6.1:** Assignment of IR bands to surface species adsorbed on $\gamma$-$Al_2O_3$ relevant for DME-SCR.

## *6.1. Surface species during DME-SCR over γ-$Al_2O_3$*

Figure 6.1 shows the DRIFT spectra obtained during the temperature programmed desorption of DME in the presence of NO in the gas phase, which is part of the study of **paper V**. The lowermost spectrum was taken after adsorption of 1000 ppm DME at 30 °C for 30 min and flushing of the sample for further 30 min. The spectrum above was obtained after holding the sample at 50 °C for 15 min. The following spectra were recorded with increments of 50 °C from 50 to 500 °C. When adsorbing DME on the catalyst surface, bands in three different regions appear where region A covers 3850-3450 $cm^{-1}$, region B 3100-2700 $cm^{-1}$ and region C

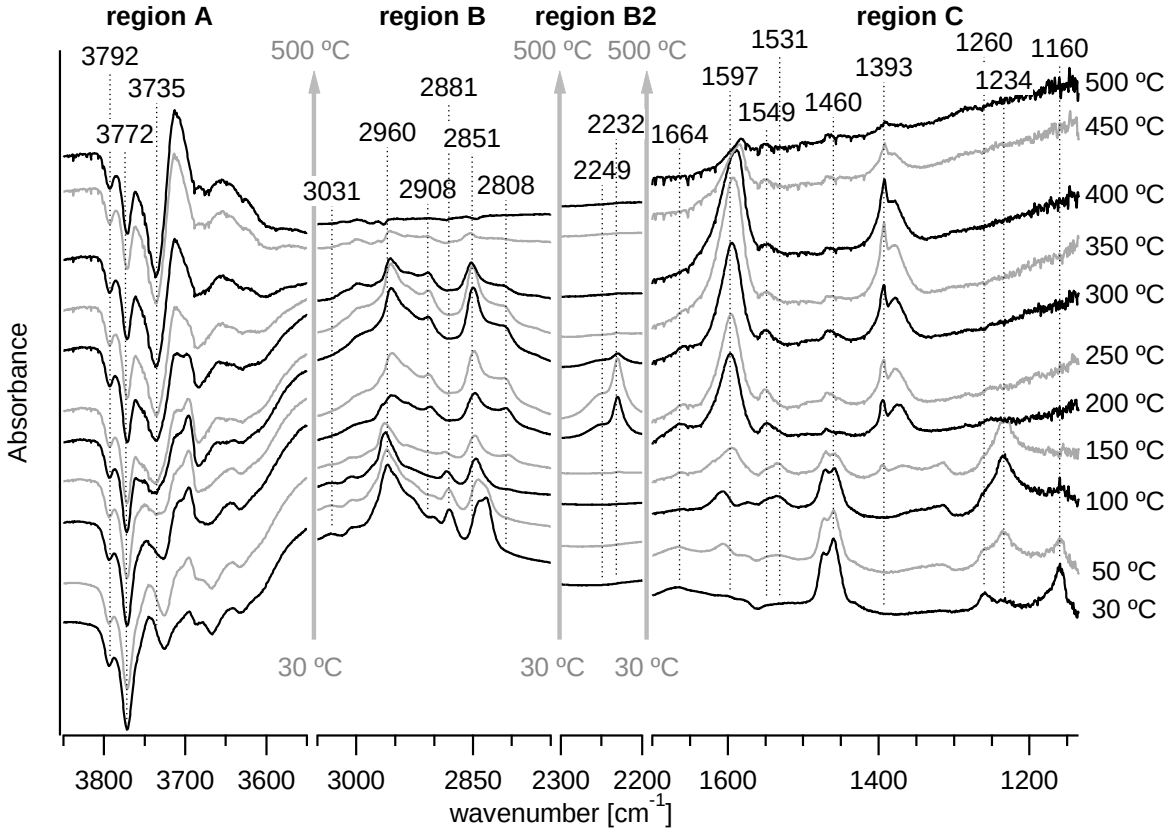


**Figure 6.1:** Surface species during temperature programmed reaction of DME in the presence of NO over $\gamma$-$Al_2O_3$.

1700-1100 $cm^{-1}$. In Figure 6.1, the negative bands in region A can all be assigned to the disappearance of different OH groups due to either interactions or reaction with adsorbed species. The positive bands in regions B and C may be due to molecularly adsorbed DME ($CH_3$-O-$CH_3$), molecularly adsorbed methanol ($CH_3OH$) or methoxy species ($CH_3O^-$). Differentiation between these species is difficult, since the similar structures cause bands at the same wavenumbers. However, only the OH-group of molecularly adsorbed methanol gives rise to a broad band around 3200 $cm^{-1}$ [40, 90], which is missing after the adsorption of DME. Therefore, the adsorption of significant amounts of molecularly adsorbed methanol can be excluded. Moreover, Chen et al. showed in a temperature programmed desorption of DME (DME-TPD) over $Al_2O_3$ bands shifting during the transformation of DME into methoxy groups between 200 and 250 K [91]. Based on these results, all positive bands in region B and C are assigned to different features of methoxy groups.

At 50 °C, in the presence of NO, a new peak appeared at 1234 $cm^{-1}$, which can be assigned to nitrite species as referenced in Table 6.1. With further increasing temperature, the methoxy peaks diminished in region C, while in region B, the peaks assigned to the C-H vibrations of the methoxy group either decreased or shifted positions when raising the temperature from 30 to 150 °C. Between 100 and 150 °C, a band is observed at 1531 $cm^{-1}$, which in **paper V** was ascribed to

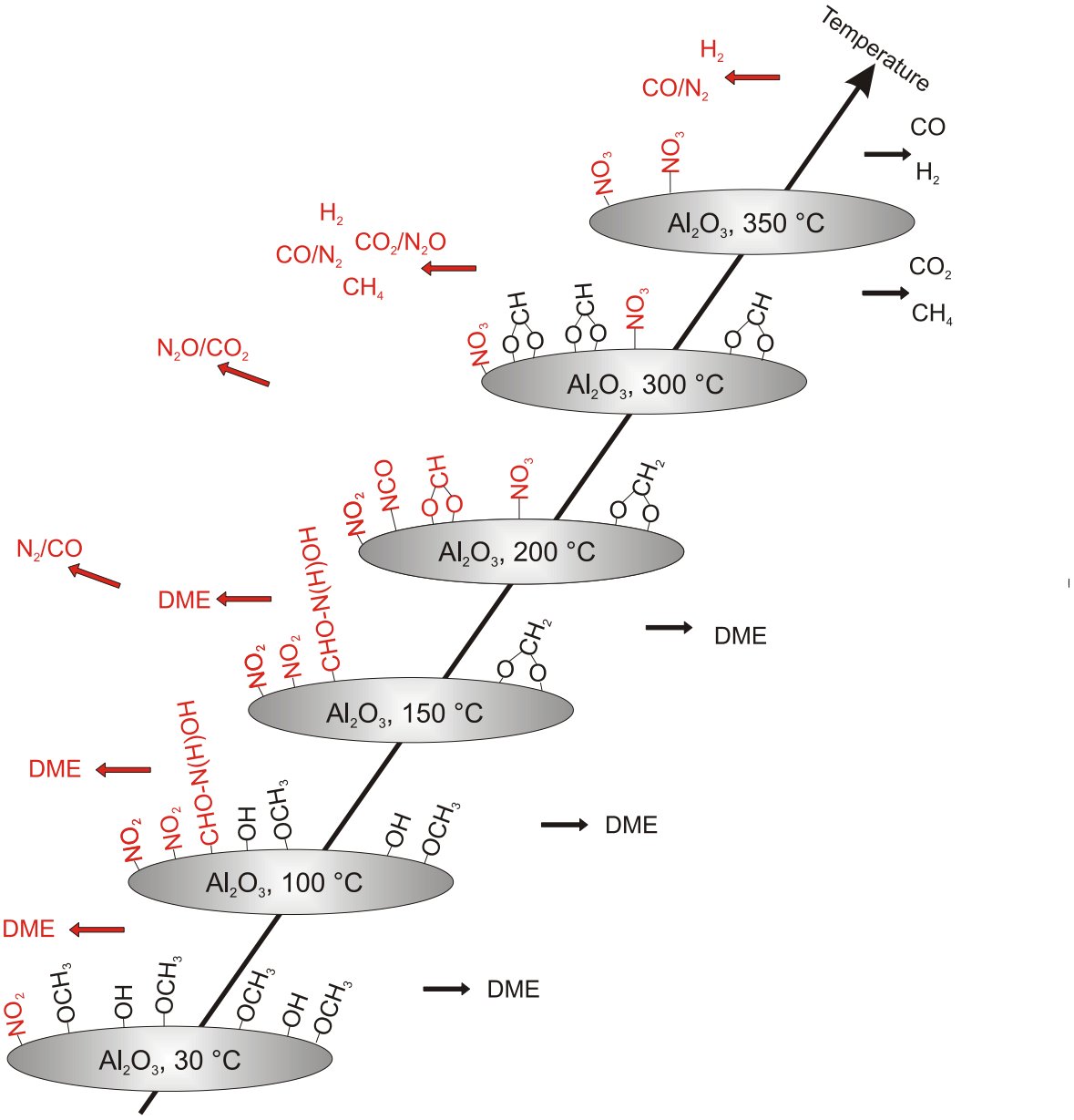


**Figure 6.2:** Possible reaction scheme of the adsorption of DME on γ-$Al_2O_3$ and subsequent temperature programmed desorption in an Ar flow (black) or in a flow of 500 ppm NO in Ar (red).

formohydroxamic acid (CHO-N(H)OH). At 150 °C, another new band appeared in region B at 2808 $cm^{-1}$, which in **paper V** was tentatively assigned to dioxymethylene species ($O\text{-}CH_2\text{-}O_2^-$), a formaldehyde-like species. Other features became clearly visible at 200 °C in region C and B2. The features in region B2 at 2249 and 2232 $cm^{-1}$ can be assigned to isocyanates (NCO) and the bands around 1597 and 1549 $cm^{-1}$ in region C to unresolved vibrations of differently bound nitrates and possibly nitrites as summarized in Table 6.1. Moreover, the bands at 1393 and 1377 $cm^{-1}$ are due to different vibrations of formate species. These peaks reached a maximum at 400 °C and disappeared at 500 °C. Similar to the nitric oxide peak at 1234 $cm^{-1}$, a peak at 1664 $cm^{-1}$ is visible already at 30 °C during the temperature programmed reaction of DME (DME-TPR) in the presence of NO. The assignment of peaks at 1664 $cm^{-1}$ is more ambiguous, as they may be due to the N-O vibration of inorganic or organic nitrites [29, 66, 107, 108] or to a species containing a C-N double bound as e.g. nitrosoaldehyde dianion ($HC(O)=NO^{2-}$) which is discussed as a precursor for NCO species [109-111]. From the abailable information, both an assignment to methylnitrites ($CH_3\text{-}ONO$) and a nitrosoaldehyde dianion are possible. Based on these observations, a scheme of the reactions occurring during a DME-TPD or DME-TPR in the presence of NO has been proposed in **paper V** and is illustrated in Figure 6.2.

## *6.2. Mechanistic considerations of DME-SCR over γ-$Al_2O_3$*

In Figure 6.3, the accumulation and consumption of surface species at 250 °C during a step response experiment with DME, NO and $O_2$ are shown. When the γ-$Al_2O_3$ sample is exposed to NO and $O_2$ during the first step, nitrates and possibly nitrites are formed as referenced in Table 6.1. In step 2, DME was added to the gas mixture, which results in the formation of methoxy species (1474 $cm^{-1}$), formate species (1377 $cm^{-1}$) and a formaldehyde-like species (2804 $cm^{-1}$). All these species have been previously discussed in the TPR with NO in Figure 6.1. In addition, more nitrates accumulate on the surface as indicated by the band at 1300 $cm^{-1}$. The intense band around 1589 $cm^{-1}$ likely comprises overlapping bands of formates, nitrates and possibly nitrites as summarized in Table 6.1. Reactions between carbon- and nitrogen-containing species are, moreover, indicated by the occurrence of NCO bands at 2257 and 2234 $cm^{-1}$. These species were stable upon the removal of the NO from the reaction mixture in step 3 and upon re-addition of it in step 4. In

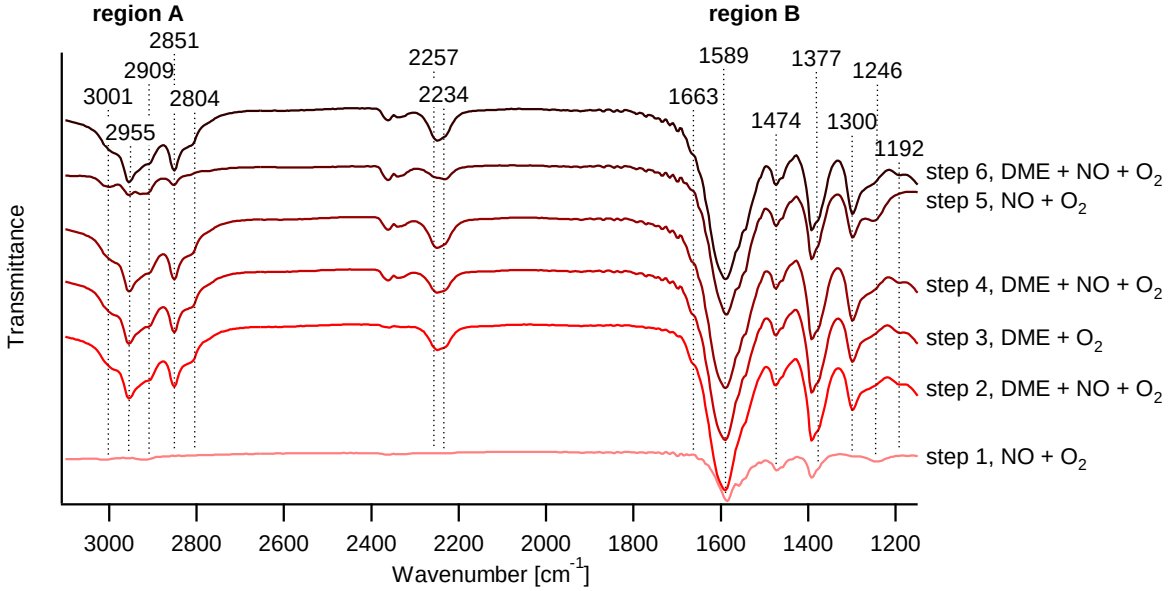


**Figure 6.3:** Step response experiment over γ-$Al_2O_3$ at 250 °C in the absence of gas phase reactions. 1000 ppm DME and 500 ppm NO in 8 % $O_2$ in Ar were sequentially added and removed from the gas mixture.

step 5, when DME is removed from the gas mixture, the hydrocarbon bands in region A diminish as well as the formate band and the NCO bands. In contrast, a nitrate band at 1246 $cm^{-1}$ grows. When DME is added again to the gas mixture in step 6, the identical absorption pattern reappeared as in steps 2 to 4.

Qualitatively, a similar evolution of bands was observed for the step response experiments performed at 350 °C in the absence of gas phase reactions and at 250 °C in the presence and absence of the gas phase reactions. Differences between these experiments can be observed in the DRIFT spectra of step 6 for the different reaction conditions employed as shown in Figure 6.4. Spectra a and b are recorded at 350 and 250 °C, respectively, in the presence of gas phase reactions. These spectra are characterised by minor bands in region A and some moderate bands in region B, which are indicative for formate species, methoxy species, nitrates and/or nitrites as referenced in Table 6.1. In the absence of gas phase reactions, all these bands are more pronounced as shown in spectra c and d. Moreover, the accumulation of isocyanate species is observed. These observations indicate that the

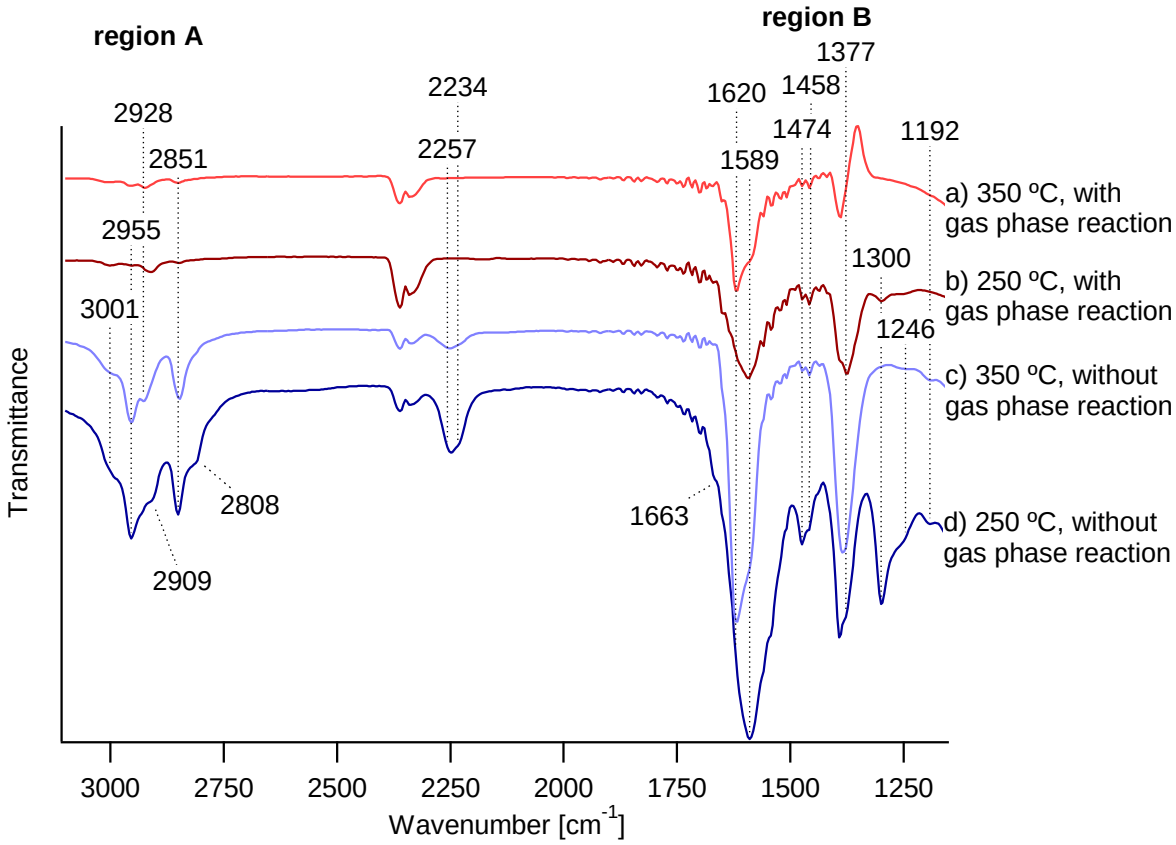


**Figure 6.4:** Surface species during DME-SCR on $\gamma$-$Al_2O_3$ at 350 °C (a,c) or 250 °C (b,d) and in the presence (a,b) or in the absence (c,d) of gas phase reactions.

presence or absence of gas phase reactions is more important for the accumulation of surface species than the temperature in these experiments. The difference in the amount of hydrocarbon species on the surface has been explained in **paper VI** by the consumption of DME in the gas phase reactions, resulting in a lower amount of hydrocarbons available on the surface. This explanation, however, does not include the differences in NCO accumulation on the surface.

For more insight into the system, the area of the NCO band is therefore plotted as a function of time for the step response experiments at 250 and 350 °C in the absence of gas phase reactions in Figure 6.5a. At 250 °C, NCO species were constantly observed during steps 2 to 6. The transient behaviour of the NCO species as a function of gas mixture will be discussed in chapter 6.3. Unexpected from the information of Figure 6.4 trace c, NCO species are not stable under reaction conditions at 350 °C as shown in Figure 6.5a. Apparently, the NCO species

accumulated when the catalyst was cooled from 350 to 250 °C. When the reaction gases subsequently met the catalyst at 350 °C, the accumulated NCO species were rapidly consumed.

The observation of accumulated NCO species at the beginning of steps 3 to 6 indicates that NCO species indeed were formed at 350 °C but rapidly consumed preventing an accumulation. In contrast, at 250 °C, NCO species accumulate during SCR reaction conditions, i.e. DME, NO and $O_2$ present, as shown in Figure 6.5a in step 2. This indicates that the formation of NCO species under SCR reaction conditions is faster than their consumption at 250 °C. According to the literature, this consumption is likely the hydrolysis of NCO with water forming ammonia and/or amines [32, 34, 112-114].

In the presence of gas phase reactions, no clear accumulation of NCO species has been detected at 250 °C. The lack of detection might be either explained by a different reaction mechanism in the presence of gas phase reactions, which does not include the formation of isocyanates; or the consumption of NCO species is accelerated hindering an accumulation on the catalyst surface and thus their detection. During the gas phase reactions, mainly $NO_2$, CO and radicals are formed as discussed in chapter 4. This change in reducing agent, however, does not explain the absence of isocyanate species, since these species have been detected with a variety of carbon containing reducing agents [29, 34, 65, 111, 115]. However, it has been reported that the activity of $Al_2O_3$ for $NO_x$ reduction increases and shifts to lower temperatures when replacing NO by $NO_2$ in the effluent stream [28, 29, 31]. In the context of the higher $NO_x$ reduction with $NO_2$ than with NO it is interesting to note that deactivation has been reported caused by accumulation of NCO species in the absence of $NO_x$ and water while $NO_2$ reacted more easily with these species [32]. In the study for paper VI, isocyanate species accumulate on the $\gamma$-$Al_2O_3$ catalyst surface at 250 °C in the absence of gas phase reactions. Moreover, $NO_x$ conversion increases in the presence of gas phase reactions at 250 °C, when no clear bands of NCO species are observed (Figure 6.4). It is thus reasonable to assume, that the $NO_2$ formed in the gas phase reactions accelerates the consumption of NCO species on the catalyst surface and thereby increases the $NO_x$ conversion at 250 °C. In contrast, at 350 °C, the reaction of NCO species is fast, but the oxidation of DME during the gas phase reactions consumes parts of the reducing agent, which limits $NO_x$ reduction.

## *6.3. Comparison of DME-SCR over γ-$Al_2O_3$ and propene-SCR over $Ag/Al_2O_3$*

Figure 6.5 is a comparison of the accumulation and consumption of isocyanate (NCO) and cyanide (CN) species on the catalyst surface during step response experiments for DME-SCR over γ-$Al_2O_3$ (a) taken from **paper VI** and propene-SCR over $Ag/Al_2O_3$ (b) taken from **paper I**. In the same figure, the formation of isocyanic acid (HNCO), hydrogen cyanide (HCN) and ammonia ($NH_3$) in the gas phase during propene-SCR conditions is presented (c). Cyanide species have not been observed for DME-SCR under any of the studied conditions.

When discussing the formation and consumption of species as a function of the gas mixture and the preceding step, the sites on which the species adsorb also need to be taken into account. Cyanide species adsorbed on silver were reported to give rise to a band around 2130 $cm^{-1}$ and CN species adsorbed on aluminum cause a band between 2165 and 2155 $cm^{-1}$ [95]. Both of these species were observed in **paper I** and were added to the band area reported in Figure 6.5. Unfortunately, a separate treatment of the peak areas of these bands is hardly possible due to a major overlap. Isocyanate species adsorbed on silver results in a band at 2204 $cm^{-1}$ and NCO species on aluminum absorb IR light around 2230 and 2255 $cm^{-1}$ [95]. In **paper I** during propene-SCR, exclusively the NCO band at 2230 $cm^{-1}$ was detected, indicating that the NCO was only adsorbed on aluminum. For the following discussion, it is therefore assumed that the reactions catalyzed by silver were not rate determining in the formation of NCO species and did not accelerate their consumption under the conditions studied.

Moreover, it is important to note that the step response experiment for propene-SCR in **paper I** was carried out at 475 °C, which is significantly higher than the temperatures studied for DME-SCR in **paper VI**. In general, an increase of bands due to an accumulation of species on the surface is caused by a faster formation than consumption and, consequently, a decrease of bands indicates a more rapid consumption than formation. Excluding formation or consumption is rarely possible.

In none of the experiments, NCO species were observed in step 1 since no hydrocarbon species were available on the catalyst surface. In step 2, DME or

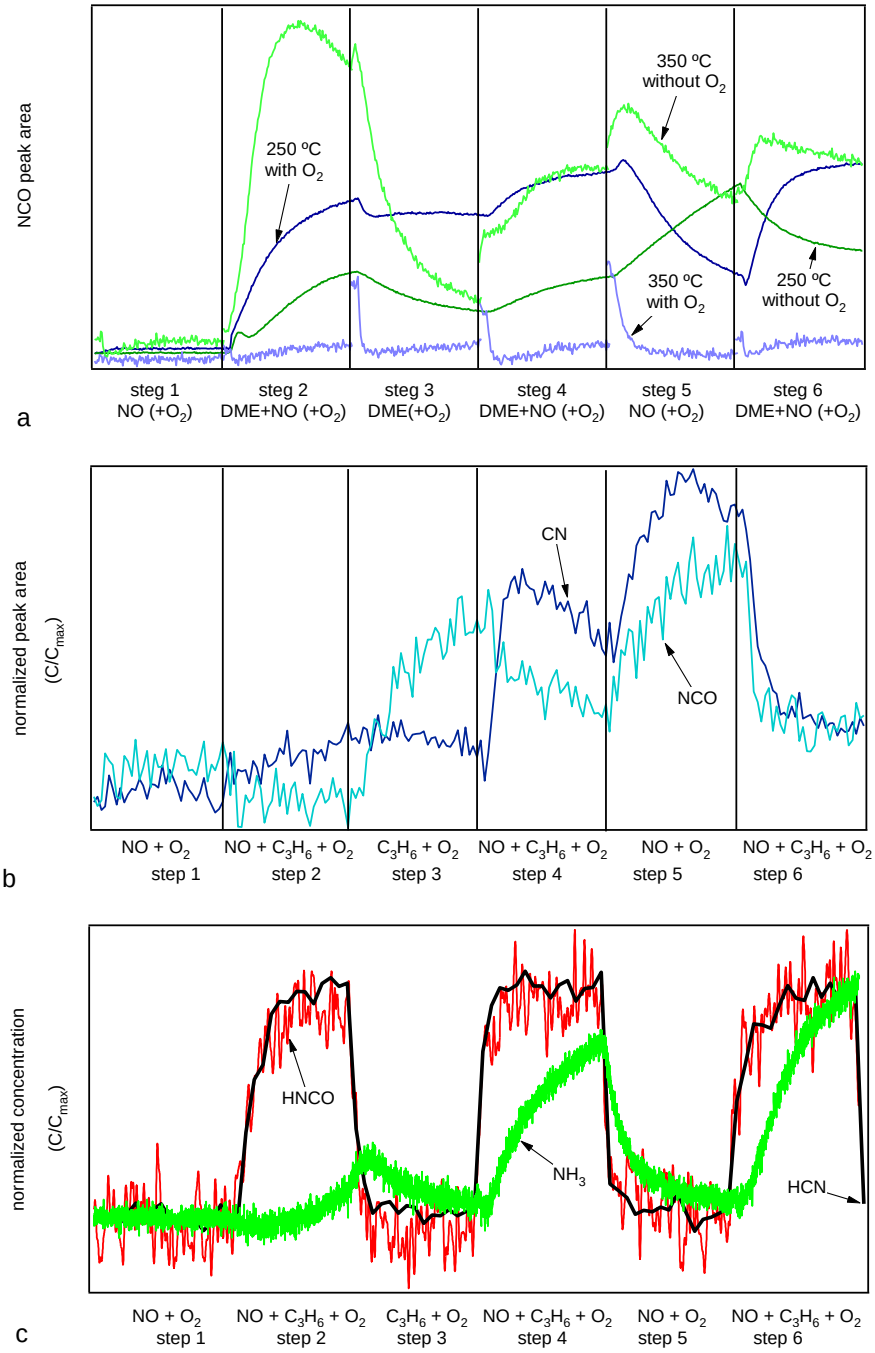


**Figure 6.5:** Evolution of (a,b) NCO and (b) CN species and (c) HCN, HNCO and $NH_3$ in the gas phase during step response experiments (a) with DME as reducing agent over γ-$Al_2O_3$ or (b,c) with propene over Ag/$Al_2O_3$. Gas mixtures: (a) 500 or (b,c) 1000 ppm NO, (a) 1000 ppm DME, (b) 1000 ppm or (c) 500 ppm $C_3H_6$ and 8 % $O_2$ balanced in Ar. Two experiments in (a) (green lines) were carried out without $O_2$.

propene were added to the gas mixture. With DME, NCO species started to accumulate at 250 and at 350 °C in the absence of oxygen, but not at 350 °C in the presence of $O_2$ as shown in Figure 6.5a. The formation and consumption of NCO species at 350 °C in the presence of $O_2$ has already been discussed in chapter 6.3 and is not covered in this chapter. No NCO species were observed during this step with propene. The different rates of accumulation at 250 °C in step 2 in the experiments with DME indicate a positive effect of $O_2$. Moreover, the more rapid accumulation at 350 than at 250 °C in the absence of $O_2$ indicates that higher temperatures also accelerate NCO formation. Given a rapid NCO formation in the presence of $O_2$ at 350 °C, NCO consumption also needs to be fast in the presence of $O_2$ at 350 °C, preventing NCO accumulation. Formation of HNCO and HCN in the gas phase as shown in Figure 6.5c indicates, moreover, that NCO and CN species were formed during propene-SCR conditions in step 2. The faster consumption of NCO species at 350 °C during DME-SCR conditions can explain that no NCO accumulated in step 2 during propene-SCR at 450 °C when assuming that silver is not directly involved in these reactions.

When removing NO from the gas stream in step 3, NCO species accumulated with propene; but with DME, the NCO bands diminished. It is likely that some water, which hydrolyzes NCO species to $NH_3$ [32, 34, 112-114], was formed under these conditions in all step response experiments performed. Since the amount of NCO species was stable after an initial decrease at 250 °C in the presence of $O_2$, the expected formation of water may indicate that NCO species were continuously formed when only DME and $O_2$ were present in the gas phase, presumably from adsorbed N-containing species. Continued formation of NCO species was also observed in the experiment with propene, where NCO species accumulated in step 3. This accumulation is unexpected from the decrease of the NCO band in the absence of $O_2$ with DME. It can, however, be explained by the faster NCO formation in the presence of $O_2$ and the higher temperature, as discussed before. Moreover, the oxidation of propene and the formation of water decreased in the absence of NO as shown in **paper I**, explaining the slower consumption at this step.

Returning to SCR conditions in step 4, NCO species accumulated on the surface with DME as reducing agent, while the absorption band of these species diminished with propene indicating that the consumption of NCO species was faster than their formation under these conditions. When removing the reducing agent from the feed

in step 5, the NCO bands initially increased followed by a considerable decrease in the presence of DME and $O_2$ at 250 °C and in the absence of $O_2$ at 350 °C. In contrast, after removing DME in the absence of $O_2$ at 250 °C and after removing propene, the NCO species continued accumulating during the whole step 5. The increase of the NCO bands after removing propene was in **paper I** explained by a slower consumption of NCO species due to less water available on the catalyst surface. The following decrease of the NCO band after removing DME in the presence of $O_2$ and at 350 °C in the absence of $O_2$ may indicate either an exhaustion of the precursor or that the precursor was replaced by another precursor from which the reaction occurred less effectively. However, the hydrocarbon source for the formation of NCO was not completely exhausted during the 20 min this step lasted, even at 350 °C in the presence of $O_2$, as indicated by a minor accumulation of NCO species in the beginning of step 6, as shown in Figure 6.5. Finally during SCR conditions, in step 6, no common trend for the NCO band was observed. In the experiment at 250 °C in the presence of $O_2$, the NCO band increased again, similar to the other steps with SCR conditions (steps 2 and 4). During propene-SCR conditions, the bands of NCO species decreased sharply in the beginning of the step and leveled out towards the end, which was also similar to the other steps with SCR conditions. With DME in the absence of $O_2$, the NCO band initially sharply increased followed by a modest decrease at 350 °C. Under the same conditions at 250 °C, the band decreased monotonically. In contrast, the NCO band mainly increased during step 2, the other step with SCR conditions which followed a step without DME. This contradictory behavior may be explained by equilibrium reactions of the surface species, since the peak area reached approximately the same level at the end of steps 4 and 6. The different peak area at the end of step 2 was thus caused by a lack of time to reach these equilibrium conditions.

The accumulation and consumption of CN species differed from that of the NCO species. No clear accumulation of CN species was observed before step 4 when returning to SCR conditions from a step with only propene and oxygen. The CN band increased sharply in the beginning of this step and then decreased toward the end. When removing propene from the gas mixture in step 5, the CN bands decreased after an initial increase. Finally, in step 6, the bands of the CN species decreased sharply in the beginning, leveling out towards the end. In contrast to the surface species, the similar detection of trace amounts of HCN in the gas phase in steps 2, 4 and 6 indicates high turnover frequencies for these species under SCR

conditions. Summarizing the conditions when CN species were formed, it is obvious that NO needed to be present in the gas phase. However, from these observations it cannot be concluded that CN is directly formed from gas phase species. Cyanide species could just as well be formed from short lived N-containing intermediates on the surface as concluded in **paper I**. Moreover, silver appears to be crucial for the formation of CN species, since no CN species where observed in the experiments on the $\gamma$-$Al_2O_3$ catalyst.

Thanks to the different reaction conditions during the step-response experiments, it was concluded that the presence of $O_2$ in the gas stream and an increase in temperature from 250 to 350 °C accelerates NCO formation. Moreover, CN species were only observed over $Ag/Al_2O_3$ catalysts, while NCO species were formed over both silver-free $\gamma$-$Al_2O_3$ and $Ag/Al_2O_3$. This supports the conclusion from **paper I** that CN is not the main precursor for NCO in our experiments. This conclusion, however, is not in accordance to a recent paper where details of the formation of NCO species from CN species adsorbed on silver particles were reported [58]. Consequently, at least two different pathways appear to exist for the formation of NCO species during HC-SCR, which may be of different importance for NCO formation over different catalysts and with different reducing agents. The reaction pathway, which appears to be most important in the experiments performed for this thesis, is supported by the reaction scheme presented in Figure 2.2.

## *6.4. Reaction mechanism for DME-SCR over $\gamma$-$Al_2O_3$*

Adding all the information from the preceding chapters and those from **papers I** to **VI** allows proposing a detailed reaction mechanism for DME-SCR over $\gamma$-$Al_2O_3$ and the processes occurring before the catalyst.

At temperatures above about 300 °C, DME dissociates into a methoxy radical ($H_3CO^{\bullet}$) and a methyl radical ($CH_3^{\bullet}$) in the gas phase which react in the presence of $O_2$ and NO in a complex network of reactions to CO, $NO_2$, formaldehyde, formic acid and nitric acid as main products (**paper II**). Moreover, nitromethane ($H_3C$-$NO_2$) and nitrosomethane ($H_3C$-NO) are formed in the gas phase according to a detailed model [76]. A $\gamma$-$Al_2O_3$ catalyst was shown to be active for $NO_x$ reduction above about 300 °C reaching a maximum conversion of 47 % at 380 °C with high selectivity to $N_2$ in a gas mixture of 1000 ppm DME, 500 ppm NO and 8 % $O_2$ balanced in Ar (**paper IV**).

On the catalyst surface, methoxy species, probably formaldehyde-like species (dioxymethylene, O-$CH_2$-$O_2^-$) and formate species are formed on the surface during the adsorption of DME (**paper V**). In parallel, nitrites and nitrates are formed through the adsorption of NO and $NO_2$ in the presence of $O_2$. It is likely that some of these species react and form nitromethane ($H_3C$-$NO_2$). In the literature, aci-nitromethane has been proposed as the first intermediate in the path from nitromethane to isocyanate over γ-$Al_2O_3$ [32, 111]. Formohydroxamic acid (CHO-N(H)OH ) is another frequently discussed intermediate in the formation of NCO species from nitromethane during hydrocarbon SCR [32, 34, 104, 113, 116]. In **paper V**, we report the observation of a band which reasonably can be assigned to formohydroxamic acid, and NCO species have been observed in **papers I, V** and **VI**. Moreover, NCO species are reported to hydrolyse with water forming $NH_3$ and/or amine species [32, 34, 112-114, 116]. For ammonia-SCR, it has been proposed that HONO reacts with ammonia to ammonium nitrite, which subsequently decomposes to $N_2$ and water over zeolite and $Al_2O_3$-based catalysts [67, 114].

The presence of gas phase reactions increases $NO_x$ conversion at 250 °C due to faster reactions between NCO species and $NO_2$ formed in the gas phase reactions. At 350 °C, however, $NO_x$ conversion is decreased due to partial oxidation of DME in the gas phase reactions, which consumes the limiting reducing agent (**paper IV**).

# 7. Concluding remarks

Dimethyl ether (DME) is one of the most energy effective and low $CO_2$ emitting alternative fuels when produced from biomass gasification [3, 4]. Due to its high cetane number DME is an interesting fuel for the diesel process [3, 5]. Similar to other vehicles with combustion engines, vehicles running on DME will most likely need after-treatment technologies for a further reduction of $NO_x$ emissions to meet most stringent upcoming legislations. One attractive technique would be selective catalytic reduction with DME (DME-SCR) as reducing agent, which was in the focus in this thesis.

It was shown that, dimethyl ether is a special reducing agent since it induces radical reactions in the gas phase before the catalyst in the presence of $O_2$ and NO above 300 °C. However, no clear reduction of $NO_x$ to $N_2$ was observed during these gas phase reactions.

Despite these conditions, good activity for $NO_x$ reduction and high selectivity to $N_2$ were achieved with DME over an H-ZSM-5 and a $\gamma$-$Al_2O_3$ catalyst. Diffuse reflectance infrared Fourier transform (DRIFT) and transmission FTIR spectroscopy experiments over $\gamma$-$Al_2O_3$ revealed the occurrence of methoxy, formate, nitrate, nitrate, NCO and likely formohydroxamic acid and formaldehyde-like species on the catalyst surface under DME-SCR conditions. Since several of these species are also discussed for conventional HC-SCR over low loaded $Ag/Al_2O_3$, we suggest, that the reaction mechanism for DME-SCR over $Al_2O_3$ is similar to that proposed for hydrocarbons over $Ag/Al_2O_3$, except for the activation steps leading to the formation of formohydroxamic acid.

Reduction of $NO_x$ starts during DME-SCR over $\gamma$-$Al_2O_3$ and H-ZSM-5 at the same temperature as the gas phase reactions indicating an important impact of the gas phase reactions on the $NO_x$ reduction. In experiments, where the occurrence of the gas phase reactions could be controlled independently of the catalyst temperature, it was shown that the formation of $NO_2$ in the gas phase reactions boost the activity for $NO_x$ reduction over $\gamma$-$Al_2O_3$ at 250 °C probably due to a more efficient reaction between $NO_2$ and NCO surface species. In contrast, at 350 °C a lower activity for $NO_x$ reduction was achieved in the presence than in the absence of the gas phase

reactions. This negative effect can be explained by a simplified view of the gas phase reactions as partial oxidation of DME decreasing the amount of the limiting reducing agent at 350 °C.

# 8. Outlook/Future work

A number of questions have not been addressed in this thesis but might be of interest for future studies.

- The activity for $NO_x$ reduction observed in this thesis needs to be increased before DME-SCR can be applied in a vehicle. This higher activity might be achieved by using alumina or ZSM-5 as a supporting material. For ZSM-5, impregnation instead of ion-exchange might result in higher activity since the acidic sites were shown to be beneficial for DME-SCR. With this background a comparison of the surface species over $\gamma$-$Al_2O_3$ and over H-ZSM-5 might also be of interest.

- An experimental set-up, where the occurrence of gas phase reactions can be controlled independently of the catalyst temperature, and which at the same time allows for the analysis of the gas composition by gas phase FTIR under transient conditions would be desirable for further studies. This can either be achieved by a gas phase FTIR cell with a smaller gas volume or a higher gas flow in the reactor.

- The influence of water both on the activity over $\gamma$-$Al_2O_3$ and on the reaction mechanism would be interesting to study. In the literature it was reported, that the activity for $NO_x$ reduction with DME was similar in the presence and absence of water over a $Ga_2O_3/Al_2O_3$ catalyst. This was explained by the same amount of adsorbed DME [37]. It would be interesting to study this phenomenon by DRIFT.

- During the study of the influence of the gas phase reactions on the surface species, the formation of NCO species was observed. When DME was removed from the gas mixture after a step with DME, NO and $O_2$ present, the formation of NCO species continued during the 20 min of each step of the experiment. It could be interesting to extent step 5 with only NO and $O_2$ in the gas mixture and examine if NCO can be formed from formates over $\gamma$-$Al_2O_3$.

- Due to the short hydrocarbon chain consisting of only one carbon atom, the DME- or methanol-SCR system should be suitable for DFT-calculations.

# 9. Acknowledgements

This work was performed within the Competence Centre for Catalysis, which is hosted by Chalmers University of Technology and financially supported by the Swedish Energy Agency and the member companies: AB Volvo, Volvo Car Corporation, Scania CV AB, Saab Automobile Powertrain AB, Haldor Topsøe A/S and the Swedish Space Corporation. It was financially supported by the Swedish Agency for Innovation Systems, Swedish Road Administration, and the Swedish Environmental Protection Agency for financial support through the EMFO program.

Many people have contributed and I want to thank especially the following people for making this thesis feasible and enjoyable:

- Professor **Krister Holmberg**, my examiner for giving me the opportunity to do research at Applied Surface Chemistry.
- Professor **Anders Palmqvist**, my main supervisor, for inspiring scientific discussions, thorough reading of all my manuscripts and the freedom in running my PhD project.
- Professor **Magnus Skoglundh**, director of the Competence Centre for Catalysis and my second supervisor, for your great enthusiasm and taking your time to help with urgent questions.
- Doctor **Hanna Härelind Ingelsten**, my third supervisor, for always being so positive, having time to discuss ideas and problems and encouraging me in difficult times.
- **Lars Lindström** for help in the lab.
- **Ann Jakobsson** for help with administrative questions.

- **Romain Bordes**, **Martin Hall** and **Per Eriksson** for help with my computer.

- **Marika Männikö** and **Per-Anders Carlsson** my roommates for lots of pleasant discussions and a nice atmosphere.

- **Malin Berggrund** for being such a good friend.

- **Friends** and **colleagues** at **KCK** and **TYK** for a nice working atmosphere which make it easy to work.

- My **family** for sharing with me what is important.

# 10. List of abbreviations

**DME** **dimethyl ether**

**DRIFT** **diffuse reflectance Fourier transform infrared**

**FTIR** **Fourier transform infrared**

**HC** **hydrocarbon**

**IR** **Infrared**

**$NO_x$** **nitrogen oxides (refers to NO and $NO_2$)**

**SCR** **selective catalytic reduction**

**TPD** **temperature programmed desorption**

**TPR** **temperature programmed reaction**

# 11. References


1. UNFCCC. *Kyoto protocol*. 2010; (targets and mechanisms of the Kyoto protocol). Available from: http://unfccc.int/kyoto_protocol/items/2830.php, accessed 2010-01-27.
2. UNFCCC. *Decision 2/CP.15*. 2009; (Decisions made during COP 15). Available from: http://unfccc.int/resource/docs/2009/cop15/eng/11a01.pdf# page=43, accessed 2010-01-28.
3. P. Ahlvik, Å. Brandberg, *Well-to-wheel efficiency for alternative fuels from natural gas and biomass*, 1st ed., Swedish National Road Administration, Borlänge, 2001, pp. 1–121, DOI: 101010, Available from: http://www.vv.se/ filer/publikationer/2001-85.pdf, accessed 2007-10-11.
4. R. Edwards, J.-F. Larivé, V. Mahieu, R. Rouveirolles, *Well-to-wheels analysis of future automotive fuels and powertrains in the European context*. 2006, Available from: http://www.co2star.eu/publications/Well_to_Tank_Report_ EU.pdf, accessed 2009-02-10.
5. Semelsberger, T.A., R.L. Borup, and H.L. Greene, *Dimethyl ether (DME) as an alternative fuel.* J. Power Sources, 2006. **156**(2): p. 497-511.
6. Akzo Nobel. *Demeon® D (Dimethyl ether)* 2010; (Producer's webpage about DME). Available from: http://www.demeon.com/, accessed 2010-01-27.
7. International DME Association. *About DME*. 2009; (DME applications). Available from: http:// www.aboutdme.org/, accessed 2010-01-28.
8. Haldor Topsoe. *DME*. (Researching business areas, Gasification-based technologies). Available from: http://www.topsoe.com/research/ Researching_ business_areas/Gasification_based/DME.aspx, accessed 2010-01-28.
9. Fleisch, T., C. McCarthy, A. Basu, C. Udovich, P. Charbonneau, W. Slodowske, S.-E. Mikkelsen, J. McCandless, *A new clean diesel technology: Demonstration of ULEV emissions on a Navistar diesel engine fueled with dimethyl ether*. Society of Automotive Engineers, 1995, Technical paper 950061
10. "nitric oxide." Encyclopædia Britannica. Encyclopædia Britannica Online. Encyclopædia Britannica, 2010. Web. 16 Apr. 2010 <http://search.eb.com/ eb/ article-9055939>.

11. "oxides of oxygen." Encyclopædia Britannica. Encyclopædia Britannica Online. Encyclopædia Britannica, 2010. Web. 16 Apr. 2010 <http://search.eb.com/eb/article-278021>.
12. "acid rain." Encyclopædia Britannica. Encyclopædia Britannica Online. Encyclopædia Britannica, 2010. Web. 16 Apr. 2010 <http://search.eb.com/eb/article-9003549>.
13. "air pollution." Encyclopædia Britannica. Encyclopædia Britannica Online. Encyclopædia Britannica, 2010. Web. 16 Apr. 2010 <http://search.eb.com/eb/article-286159>.
14. European Commission. *Transport & Environment*. (Emission regulation and directives). Available from: http://ec.europa.eu/environment/air/transport/road.htm, accessed 2010-01-27.
15. DieselNet. *Emission Standards*. 2010; Available from: http://www.dieselnet.com/standards/, accessed 2010-01-28.
16. Jobson, E., *Future challenges in automotive emission control.* Top. Catal., 2004. **28**(1-4): p. 191-199.
17. Yahiro, H. and M. Iwamoto, *Copper ion-exchanged zeolite catalysts in de$NO_x$ reaction.* Appl. Catal. A, 2001. **222**(1-2): p. 163-181.
18. Traa, Y., B. Burger, and J. Weitkamp, *Zeolite-based materials for the selective catalytic reduction of $NO_x$ with hydrocarbons.* Micropor. Mesopor. Mater., 1999. **30**(1): p. 3-41.
19. Matsumoto, S.i., *Catalytic reduction of nitrogen oxides in automotive exhaust containing excess oxygen by $NO_x$ storage-reduction catalyst.* CATTECH, 2000. **4**(2): p. 102-109.
20. Takahashi, N., H. Shinjoh, T. Iijima, T. Suzuki, K. Yamazaki, K. Yokota, H. Suzuki, N. Miyoshi, S. Matsumoto, T. Tanizawa, T. Tanaka, S. Tateishi, K. Kasahara, *The new concept 3-way catalyst for automotive lean-burn engine: $NO_x$ storage and reduction catalyst.* Catal. Today, 1996. **27**(1-2): p. 63-69.
21. Erkfeldt, S., A.E.C. Palmqvist, and E. Jobson, *$NO_x$ reduction performance of lean $NO_x$ catalyst and lean $NO_x$ adsorber using DME as reducing agent.* Top. Catal., 2007. **42-43**(1-4): p. 149-152.
22. Ritscher, J.S. and M.R. Sandner, *Three-way catalytic process for gaseous streams.*, US Patent 4297328, assigned to Union Carbide Corporation. 27 October 1981.

23. Iwamoto, M., H. Yahiro, Y. YU-U, S. Shundo, N. Mizuno, *Selective reduction of NO by lower hydrocarbons in the presence of $O_2$ and $SO_2$ over copper ion-exchanged zeolites.* Shokubai, 1990. **32**(6): p. 430-433.
24. Held, W., A. König, T. Richter, L. Puppe, *Catalytic $NO_x$ reduction in net oxidizing exhaust gas*. Society of Automotive Engineers, 1990, Technical paper 900496.
25. Burch, R., J.P. Breen, and F.C. Meunier, *A review of the selective reduction of $NO_x$, with hydrocarbons under lean-burn conditions with non-zeolitic oxide and platinum group metal catalysts.* Appl. Catal. B: Environ., 2002. **39**(4): p. 283-303.
26. Miyadera, T., *Alumina-supported silver catalysts for the selective reduction of nitric oxide with propene and oxygen-containing organic compounds.* Appl. Catal. B: Environ., 1993. **2**(2-3): p. 199-205.
27. Montreuil, C.N. and M. Shelef, *Selective reduction of nitric-oxide over Cu-ZSM-5 zeolite by water-soluble oxygen-containing organic-compounds.* Appl. Catal. B: Environ., 1992. **1**(1): p. L1-L8.
28. Hamada, H., Y. Kintaichi, M. Sasaki, T. Ito, M. Tabata, *Selective reduction of nitrogen monoxide with propane over alumina and H-ZSM-5 zeolite - Effect of oxygen and nitrogen-dioxide intermediate.* Appl. Catal., 1991. **70**(2): p. L15-L20.
29. Meunier, F.C., J.P. Breen, V. Zuzaniuk, M. Olsson, J.R.H. Ross, *Mechanistic aspects of the selective reduction of NO by propene over alumina and silver-alumina catalysts.* J. Catal., 1999. **187**(2): p. 493-505.
30. Masters, S.G. and D. Chadwick, *Selective reduction of nitric oxide by methanol and dimethyl ether over promoted alumina catalysts in excess oxygen.* Appl. Catal. B: Environ., 1999. **23**(4): p. 235-246.
31. Bethke, K.A. and H.H. Kung, *Supported Ag catalysts for the lean reduction of NO with $C_3H_6$.* J. Catal., 1997. **172**(1): p. 93-102.
32. Cowan, A.D., N.W. Cant, B.S. Haynes, P.F. Nelson, *The catalytic chemistry of nitromethane over Co-ZSM-5 and other catalysts in connection with the methane-$NO_x$ SCR reaction.* J. Catal., 1998. **176**(2): p. 329-343.
33. Hamada, H., Y. Kintaichi, M. Inaba, M. Tabata, T. Yoshinari, H. Tsuchida, *Role of supported metals in the selective reduction of nitrogen monoxide with hydrocarbons over metal/alumina catalysts.* Catal. Today, 1996. **29**(1-4): p. 53-57.

34. Zuzaniuk, V., F.C. Meunier, and J.R.H. Ross, *Differences in the reactivity of organo-nitro and nitrito compounds over $Al_2O_3$-based catalysts active for the selective reduction of $NO_x$.* J. Catal., 2001. **202**(2): p. 340-353.
35. Iglesias-Juez, A., M. Fernandez-Garcia, A. Martinez-Arias, Z. Schay, Z. Koppany, A.B. Hungria, A. Fuerte, J.A. Anderson, J.C. Conesa, J. Soria, *Catalytic properties of $Ag/Al_2O_3$ catalysts for lean $NO_x$ reduction processes and characterisation of active silver species.* Top. Catal., 2004. **30-31**(1-4): p. 65-70.
36. Masuda, K., K. Tsujimura, K. Shinoda, T. Kato, *Silver-promoted catalyst for removal of nitrogen oxides from emission of diesel engines.* Appl. Catal. B: Environ., 1996. **8**(1): p. 33-40.
37. Miyahara, Y., M. Takahashi, T. Masuda, S. Imamura, H. Kanai, S. Iwamoto, T. Watanabe, M. Inoue, *Selective catalytic reduction of NO with C1-C3 reductants over solvothermally prepared $Ga_2O_3/Al_2O_3$ catalysts: Effects of water vapor and hydrocarbon uptake.* Appl. Catal. B: Environ., 2008. **84**(1-2): p. 289-296.
38. Alam, M., O. Fujita, and K. Ito, *Performance of $NO_x$ reduction catalysts with simulated dimethyl ether diesel engine exhaust gas.* Proc. Inst. Mech. Eng. Part A: J. Power Energy, 2004. **218**(A2): p. 89-95.
39. Ozensoy, E., D. Herling, and J. Szanyi, *$NO_x$ reduction on a transition metal-free $\gamma$-$Al_2O_3$ catalyst using dimethyl ether (DME).* Catal. Today, 2008. **136**(1-2): p. 46-54.
40. Busca, G., P.F. Rossi, V. Lorenzelli, M. Benaissa, J. Travert, J.C. Lavalley, *Microcalorimetric and fourier-transform infrared spectroscopic studies of methanol adsorption on $Al_2O_3$.* J. Phys. Chem., 1985. **89**(25): p. 5433-5439.
41. Wu, Q., H. He, and Y.B. Yu, *In situ DRIFTS study of the selective reduction of $NO_x$ with alcohols over $Ag/Al_2O_3$ catalyst: Role of surface enolic species.* Appl. Catal. B: Environ., 2005. **61**(1-2): p. 107-113.
42. Park, J.W., C. Potvin, and G. Djega-Mariadassou, *de$NO_x$ reduction by methanol over Co/alumina.* Top. Catal., 2007. **42-43**(1-4): p. 259-262.
43. Shimizu, K., A. Satsuma, and T. Hattori, *Catalytic performance of $Ag$-$Al_2O_3$ catalyst for the selective catalytic reduction of NO by higher hydrocarbons.* Appl. Catal. B: Environ., 2000. **25**(4): p. 239-247.
44. Shimizu, K., J. Shibata, H. Yoshida, A. Satsuma, T. Hattori, *Silver-alumina catalysts for selective reduction of NO by higher hydrocarbons: structure of*

*active sites and reaction mechanism.* Appl. Catal. B: Environ., 2001. **30**(1-2): p. 151-162.

45. Lindfors, L.E., K. Eränen, F. Klingstedt, D.Y. Murzin, *Silver/alumina catalyst for selective catalytic reduction of $NO_x$ to $N_2$ by hydrocarbons in diesel powered vehicles.* Top. Catal., 2004. **28**(1-4): p. 185-189.
46. Arve, K., K. Svennerberg, F. Klingstedt, K. Eränen, L. Wallenberg, J. Bovin, L. Capek, D. Murzin, *Structure-activity relationship in HC-SCR of $NO_x$, by TEM, $O_2$-chemisorption, and EDXS study of $Ag/Al_2O_3$.* J. Phys. Chem. B, 2006. **110**(1): p. 420-427.
47. Miyadera, T., *Selective reduction of nitric oxide with ethanol over an alumina-supported silver catalyst.* Appl. Catal. B: Environ., 1997. **13**(2): p. 157-165.
48. Arve, K., F. Klingstedt, K. Eränen, D.Y. Murzin, L. Capek, J. Dedecek, Z. Sobalik, B. Wichterlova, K. Svennerberg, L.R. Wallenberg, J.O. Bovin, *Analysis of the state and size of silver on alumina in effective removal of $NO_x$ from oxygen rich exhaust gas.* J. Nanosci. Nanotechnol., 2006. **6**(4): p. 1076-1083.
49. Bion, N., J. Saussey, M. Haneda, M. Daturi, *Study by in situ FTIR spectroscopy of the SCR of NO, by ethanol on $Ag/Al_2O_3$ - Evidence of the role of isocyanate species.* J. Catal., 2003. **217**(1): p. 47-58.
50. Mhadeshwar, A.B., B.H. Winkler, B. Eiteneer, D. Hancu, *Microkinetic modeling for hydrocarbon (HC)-based selective catalytic reduction (SCR) of $NO_x$ on a silver-based catalyst.* Appl. Catal. B: Environ., 2009. **89**(1-2): p. 229-238.
51. He, H. and Y.B. Yu, *Selective catalytic reduction of $NO_x$ over $Ag/Al_2O_3$ catalyst: from reaction mechanism to diesel engine test.* Catal. Today, 2005. **100**(1-2): p. 37-47.
52. Sumiya, S., M. Saito, H. He, Q.C. Feng, N. Takezawa, K. Yoshida, *Reduction of lean $NO_x$ by ethanol over $Ag/Al_2O_3$ catalysts in the presence of $H_2O$ and $SO_2$.* Catal. Lett., 1998. **50**(1-2): p. 87-91.
53. Masters, S.G. and D. Chadwick, *Effect of $SO_2$ on selective catalytic reduction of NO by $CH_3OCH_3$ over gamma-alumina in excess oxygen.* Catal. Lett., 1999. **61**(1-2): p. 65-69.
54. Meunier, F.C. and J.R.H. Ross, *Effect of ex situ treatments with $SO_2$ on the activity of a low loading silver-alumina catalyst for the selective reduction of NO and $NO_2$ by propene.* Appl. Catal. B: Environ., 2000. **24**(1): p. 23-32.

55. Breen, J.P., R. Burch, C. Hardacre, C.J. Hill, B. Krutzsch, B. Bandl-Konrad, E. Jobson, L. Cider, P.G. Blakeman, L.J. Peace, M.V. Twigg, M. Preis, M. Gottschling, *An investigation of the thermal stability and sulphur tolerance of Ag/gamma-$Al_2O_3$ catalysts for the SCR of $NO_x$ with hydrocarbons and hydrogen.* Appl. Catal. B: Environ., 2007. **70**(1-4): p. 36-44.
56. Brosius, R. and J.A. Martens, *Reaction mechanisms of lean-burn hydrocarbon SCR over zeolite catalysts.* Top. Catal., 2004. **28**(1-4): p. 119-130.
57. Pârvulescu, V.I., P. Grange, and B. Delmon, *Catalytic removal of NO.* Catal. Today, 1998. **46**(4): p. 233-316.
58. Thibault-Starzyk, F., E. Seguin, S. Thomas, M. Daturi, H. Arnolds, D.A. King, *Real-time infrared detection of cyanide flip on silver-alumina $NO_x$ removal catalyst.* Science, 2009. **324**(5930): p. 1048-1051.
59. Inaba, M., Y. Kintaichi, and H. Hamada, *Cooperative effect of platinum and alumina for the selective reduction of nitrogen monoxide with propane.* Catal. Lett., 1996. **36**(3-4): p. 223-227.
60. Burch, R. and T.C. Watling, *The difference between alkanes and alkenes in the reduction of NO by hydrocarbons over Pt catalysts under lean-burn conditions.* Catal. Lett., 1997. **43**(1-2): p. 19-23.
61. Hadjiivanov, K., J. Saussey, J.L. Freysz, J.C. Lavalley, *FT-IR study of $NO+O_2$ co-adsorption on H-ZSM-5: re-assignment of the 2133 $cm^{-1}$ band to $NO^+$ species.* Catal. Lett., 1998. **52**(1-2): p. 103-108.
62. Koppenol, W.H., *Names for inorganic radicals.* IUPAC, Pure Appl. Chem., 2000. **72**(3): p. 437–446.
63. Iglesias-Juez, A., A.B. Hungria, A. Martinez-Arias, A. Fuerte, M. Fernandez-Garcia, J.A. Anderson, J.C. Conesa, J. Soria, *Nature and catalytic role of active silver species in the lean $NO_x$ reduction with $C_3H_6$ in the presence of water.* J. Catal., 2003. **217**(2): p. 310-323.
64. Kameoka, S., T. Chafik, Y. Ukisu, T. Miyadera, *Reactivity of surface isocyanate species with NO, $O_2$ and $NO+O_2$ in selective reduction of $NO_x$ over Ag/$Al_2O_3$ and $Al_2O_3$ catalysts.* Catal. Lett., 1998. **55**(3-4): p. 211-215.
65. Obuchi, A., C. Wögerbauer, R. Köppel, A. Baiker, *Reactivity of nitrogen containing organic intermediates in the selective catalytic reduction of $NO_x$ with organic compounds: A model study with tert-butyl substituted nitrogen compounds.* Appl. Catal. A, 1998. **19**(1): p. 9-22.

66. Sumiya, S., H. He, A. Abe, N. Takezawa, K. Yoshida, *Formation and reactivity of isocyanate (NCO) species on $Ag/Al_2O_3$.* J. Chem. Soc. Faraday Trans., 1998. **94**(15): p. 2217-2219.
67. Yeom, Y.H., J. Henao, M.J. Li, W.M.H. Sachtler, E. Weitz, *The role of NO in the mechanism of $NO_x$ reduction with ammonia over a BaNa-Y catalyst.* J. Catal., 2005. **231**(1): p. 181-193.
68. Sun, Q., Z.X. Gao, H.Y. Chen, W.M.H. Sachtler, *Reduction of $NO_x$ with ammonia over Fe/MFI: Reaction mechanism based on isotopic labeling.* J. Catal., 2001. **201**(1): p. 89-99.
69. Nova, I., C. Ciardelli, E. Tronconi, D. Chatterjee, B. Bandl-Konrad, *$NH_3$-$NO/NO_2$ chemistry over V-based catalysts and its role in the mechanism of the Fast SCR reaction.* Catal. Today, 2006. **114**(1): p. 3-12.
70. Dagaut, P., C. Daly, J. Simmie, M. Cathonnet, *The oxidation and ignition of dimethyl ether from low to high temperature (500-1600 K): Experiments and kinetic modelling.* Proceedings of the 27th Symposium (International) on Combustion/The Combustion Institute, 1998: p. 361-369.
71. Liu, I., N.W. Cant, J.H. Bromly, F.J. Barnes, P.F. Nelson, B.S. Haynes, *Formate species in the low-temperature oxidation of dimethyl ether.* Chemosphere, 2001. **42**(5-7): p. 583-589.
72. Zhao, Z., M. Chaos, A. Kazakov, F.L. Dryer, *Thermal decomposition reaction and a comprehensive kinetic model of dimethyl ether.* Int. J. Chem. Kinet., 2008. **40**(1): p. 1-18.
73. Andersen, A. and E.A. Carter, *Hybrid density functional theory predictions of low-temperature dimethyl ether combustion pathways. II. Chain-branching energetics and possible role of the Criegee intermediate.* J. Phys. Chem. A, 2003. **107**(44): p. 9463-9478.
74. Sehested, J., T. Møgelberg, T.J. Wallington, E.W. Kaiser, O.J. Nielsen, *Dimethyl ether oxidation: Kinetics and mechanism of $CH_3OCH_2 + O_2$ Reaction at 296 K and 0.38-940 Torr total pressure.* J. Phys. Chem., 1996. **100**(46): p. 17218-17225.
75. Rosado-Reyes, C.M., J.S. Francisco, J.J. Szente, M.M. Maricq, L.F. Ostergaard, *Dimethyl ether oxidation at elevated temperatures (295-600 K).* J. Phys. Chem. A, 2005. **109**(48): p. 10940-10953.
76. Dagaut, P., J. Luche, and M. Cathonnet, *The low temperature oxidation of DME and mutual sensitization of the oxidation of DME and nitric oxide:*

*Experimental and detailed kinetic modeling.* Combust. Sci.Tech., 2001. **165**: p. 61-84.

77. Langer, S., E. Ljungstrom, T. Ellermann, O.J. Nielsen, J. Sehested, *UV Absorption-Spectrum of $CH_3OCH_2$ radicals and kinetics of the reaction of $CH_3OCH_2O_2$ Radicals with NO and $NO_2$ in the gas-phase.* Chem. Phys. Lett., 1995. **240**(1-3): p. 53-56.
78. Smith, J., J. Phillips, A. Graham, R. Steele, A. Redondo, J. Coons, *Homogeneous chemistry in lean-burn exhaust mixtures.* J. Phys. Chem., 1997. **101**: p. 9157-9162.
79. Roine, A., *Outokumpu HSC Chemistry for Windows 4.0*, Chemical reaction and equilibrium software with extensive thermochemical database, Outokumpu Research Oy, Pori, Finland.
80. Ingelsten, H.H., D.M. Zhao, A. Palmqvist, M. Skoglundh, *Mechanistic study of the influence of surface acidity on lean $NO_2$ reduction by propane in H-ZSM-5*. J. Catal., 2005. **232**(1): p. 68-79.
81. Campbell, S.M., X.Z. Jiang, and R.F. Howe, *Methanol to hydrocarbons: spectroscopic studies and the significance of extra-framework aluminium.* Micropor. Mesopor. Mater., 1999. **29**(1-2): p. 91-108.
82. Forester, T.R. and R.F. Howe, *In situ FTIR studies of methanol and dimethyl ether in ZSM-5.* J. Am. Chem. Soc., 1987. **109**(17): p. 5076-5082.
83. Schnabel, K.-H., E. Schreier, and C. Peuker, *In situ FTIR studies on the conversion of methanol over acidic forms of various zeolites.* Catal. Today, 1988. **3**(5): p. 513-518.
84. Eränen, K., L.E. Lindfors, F. Klingstedt, D.Y. Murzin, *Continuous reduction of NO with octane over a silver/alumina catalyst in oxygen-rich exhaust gases: combined heterogeneous and surface-mediated homogeneous reactions.* J. Catal., 2003. **219**(1): p. 25-40.
85. Schiffino, R.S. and R.P. Merrill, *A mechanistic study of the methanol dehydration reaction on gamma-alumina catalyst.* J. Phys. Chem., 1993. **97**(24): p. 6425-6435.
86. Matyshak, V.A., L.A. Berezina, O.N. Sil'chenkova, V.F. Tret'yakov, G.I. Lin, A.Y. Rozovskii, *Properties of surface compounds in methanol conversion on gamma-$Al_2O_3$: Data of in situ IR spectroscopy.* Kinet. Catal., 2009. **50**(1): p. 111-121.

87. Matyshak, V.A., T.I. Khomenko, G.I. Lin, I.N. Zavalishin, A.Y. Rozovskii, *Surface species in the methyl formate-methanol-dimethyl ether- γ-$Al_2O_3$ system studied by in situ IR spectroscopy.* Kinet. Catal., 1999. **40**(2): p. 269-274.
88. Digne, M., P. Sautet, P. Raybaud, P. Euzen, H. Toulhoat, *Use of DFT to achieve a rational understanding of acid-basic properties of gamma-alumina surfaces.* J. Catal., 2004. **226**(1): p. 54-68.
89. Knözinger, H. and P. Ratnasamy, *Catalytic aluminas - Surface models and characterization of surface sites.* Catal. Rev. Sci. Eng., 1978. **17**(1): p. 31-70.
90. Rossi, P.F., G. Busca, and V. Lorenzelli, *Adsorption of methanol on alumina in the 298-473 K temperature-range - A microcalorimetric and FTIR spectroscopic study.* Z. Phys. Chem. N. F., 1986. **149**: p. 99-111.
91. Chen, J.G., P. Basu, T.H. Ballinger, J.T. Yates, *A transmission infrared spectroscopic investigation of the reaction of dimethyl ether with alumina surfaces.* Langmuir, 1989. **5**(2): p. 352-356.
92. Sazama, P., L. Čapek, H. Drobná, Z. Sobalík, J. Dědeček, K. Arve, B. Wichterlová, *Enhancement of decane-SCR-$NO_x$ over Ag/alumina by hydrogen. Reaction kinetics and in situ FTIR and UV-vis study.* J. Catal., 2005. **232**(2): p. 302-317.
93. McInroy, A.R., D.T. Lundie, J.M. Winfield, C.C. Dudman, P. Jones, D. Lennon, *The application of diffuse reflectance infrared spectroscopy and temperature-programmed desorption to investigate the interaction of methanol on eta-alumina.* Langmuir, 2005. **21**(24): p. 11092-11098.
94. Burch, R., J.P. Breen, C.J. Hill, B. Krutzsch, B. Konrad, E. Jobson, L. Cider, K. Eränen, F. Klingstedt, L.E. Lindfors, *Exceptional activity for $NO_x$ reduction at low temperatures using combinations of hydrogen and higher hydrocarbons on Ag/$Al_2O_3$ catalysts.* Top. Catal., 2004. **30-31**(1-4): p. 19-25.
95. Bion, N., J. Saussey, C. Hedouin, T. Seguelong, M. Daturi, *Evidence by in situ FTIR spectroscopy and isotopic effect of new assignments for isocyanate species vibrations on Ag/$Al_2O_3$.* Phys. Chem. Chem. Phys., 2001. **3**(21): p. 4811-4816.
96. Gao, H.W. and H. He, *Conformational analysis and comparison between theoretical and experimental vibration spectra for isocyanate species on Ag/$Al_2O_3$ catalyst.* Spectrochim. Acta A, 2005. **61**(6): p. 1233-1238.
97. Hadjiivanov, K.I., *Identification of neutral and charged $N_xO_y$ surface species by IR spectroscopy.* Catal. Rev. Sci. Eng., 2000. **42**(1-2): p. 71-144.

98. Martinez-Arias, A., M. Fernandez-Garcia, A. Iglesias-Juez, J.A. Anderson, J.C. Conesa, J. Soria, *Study of the lean $NO_x$ reduction with $C_3H_6$ in the presence of water over silver/alumina catalysts prepared from inverse microemulsions.* Appl. Catal. B: Environ., 2000. **28**(1): p. 29-41.
99. Wichterlová, B., P. Sazama, J.P. Breen, R. Burch, C.J. Hill, L. Čapek, Z. Sobalík, *An in situ UV–vis and FTIR spectroscopy study of the effect of $H_2$ and CO during the selective catalytic reduction of nitrogen oxides over a silver alumina catalyst.* J. Catal., 2005. **235**(1): p. 195-200.
100. Kameoka, S., Y. Ukisu, and T. Miyadera, *Selective catalytic reduction of $NO_x$ with $CH_3OH$, $C_2H_5OH$ and $C_3H_6$ in the presence of $O_2$ over $Ag/Al_2O_3$ catalyst: Role of surface nitrate species.* Phys. Chem. Chem. Phys., 2000. **2**(3): p. 367-372.
101. Shimizu, K., H. Kawabata, A. Satsuma, T. Hattori, *Role of acetate and nitrates in the selective catalytic reduction of NO by propene over alumina catalyst as investigated by FTIR.* J. Phys. Chem. B, 1999. **103**(25): p. 5240-5245.
102. Yeom, Y.H., B. Wen, W.M.H. Sachtler, E. Weitz, *$NO_x$ reduction from diesel emissions over a nontransition metal zeolite catalyst: A mechanistic study using FTIR spectroscopy.* J. Phys. Chem. B, 2004. **108**(17): p. 5386-5404.
103. Satsuma, A. and K. Shimizu, *In situ FTIR study of selective catalytic reduction of NO over alumina-based catalysts.* Progr. Energy Combust. Sci., 2003. **29**(1): p. 71-84.
104. Meunier, F.C., V. Zuzaniuk, J.P. Breen, M. Olsson, J.R.H. Ross, *Mechanistic differences in the selective reduction of NO by propene over cobalt- and silver-promoted alumina catalysts: kinetic and in situ DRIFTS study.* Catal. Today, 2000. **59**(3-4): p. 287-304.
105. Wang, J., H. He, Q.C. Feng, Y.B. Yu, K. Yoshida, *Selective catalytic reduction of $NO_x$ with $C_3H_6$ over an $Ag/Al_2O_3$ catalyst with a small quantity of noble metal.* Catal. Today, 2004. **93-95**: p. 783-789.
106. Zhang, X.L., H. He, and Z.C. Ma, *Hydrogen promotes the selective catalytic reduction of $NO_x$ by ethanol over $Ag/Al_2O_3$.* Chem. Commun., 2007. **8**(2): p. 187-192.
107. Sadykov, V.A., V.V. Lunin, V.A. Matyshak, E.A. Paukshtis, A.Y. Rozovskii, N.N. Bulgakov, J.R.H. Ross, *The reaction mechanism of selective catalytic reduction of nitrogen oxides by hydrocarbons in excess oxygen: Intermediates,*

*their reactivity, and routes of transformation.* Kinet. Catal., 2003. **44**(3): p. 379-400.

108. Tanaka, T., T. Okuhara, and M. Misono, *Intermediacy of organic nitro and nitrite surface species in selective reduction of nitrogen monoxide by propene in the presence of excess oxygen over silica-supported platinum.* Appl. Catal. B: Environ., 1994. **4**(1): p. L1-L9.
109. Ukisu, Y., S. Sato, G. Muramatsu, K. Yoshida, *Surface isocyanate intermediate formed during the catalytic reduction of nitrogen-oxide in the presence of oxygen and propylene.* Catal. Lett., 1991. **11**(2): p. 177-181.
110. Unland, M.L., *Isocyanate intermediates in reaction NO+CO over a Pt-$Al_2O_3$ catalyst.* J. Phys. Chem., 1973. **77**(16): p. 1952-1956.
111. Yamaguchi, M., *Decomposition of adsorbed nitromethane on gamma-alumina.* J. Chem. Soc. Faraday Trans., 1997. **93**(19): p. 3581-3586.
112. Ingelsten, H.H. and M. Skoglundh, *Mechanistic study of lean $NO_2$ reduction by propane over H-ZSM-5 in the presence of water.* Catal. Lett., 2006. **106**(1-2): p. 15-19.
113. Nanba, T., A. Obuchi, Y. Sugiura, C. Kouno, J. Uchisawa, S. Kushiyama, *Product analysis of selective catalytic reduction of $NO_2$ with $C_2H_4$ over H-ferrierite.* J. Catal., 2002. **211**(1): p. 53-63.
114. Yeom, Y., M. Li, A. Savara, W.M.H. Sachtler, E. Weitz, *An overview of the mechanisms of $NO_x$ reduction with oxygenates over zeolite and $\gamma$-alumina catalysts.* Catal. Today, 2008. **136**(1-2): p. 55-63.
115. Kameoka, S., T. Chafik, Y. Ukisu, T. Miyadera, *Role of organic nitro compounds in selective reduction of $NO_x$ with ethanol over different supported silver catalysts.* Catal. Lett., 1998. **51**(1 - 2): p. 11.
116. Cant, N.W. and I.O.Y. Liu, *The mechanism of the selective reduction of nitrogen oxides by hydrocarbons on zeolite catalysts.* Catal. Today, 2000. **63**(2-4): p. 133-146.